Climate change projections over Indus basin using CMIP6 model simulations

KOTESWARARAO KUNDETI (koteswararao.kundeti@apu.edu.in)
Azim Premji University
Lakshmi Kumar T.V
SRM-RI: SRM Research Institute Kattankulathur
Ashwini Kulkarni
IITM: Indian Institute of Tropical Meteorology
Chowdary J.S
IITM: Indian Institute of Tropical Meteorology
Srinivas Desamsetti
National Centre for Medium Range Weather Forecasting

Research Article

Keywords: CMIP6, Multi-Model Mean, Shared Socioeconomic Pathways, Extreme Indices

Posted Date: April 8th, 2021

DOI: https://doi.org/10.21203/rs.3.rs-365154/v1

Abstract

Indus basin is one of the most vulnerable regions due to climate change. This article presents the projected changes in precipitation and temperature over the Indus Basin using statistically downscaled, bias-corrected Coupled Model Intercomparison Project-6 (CMIP6) data sets for different shared socioeconomic pathways (SSP2-4.5 and SSP5-8.5) in response to global warming. The future changes in precipitation and temperature extremes for different epochal periods of the 21st century are outlined. The spatial variations of precipitation, maximum and minimum temperature obtained from the Multi-Model Mean (MMM) of CMIP6 models showed a good agreement with observations such as APHRODITE (precipitation), CPC (temperature) for the base period 1995 to 2014 over the Indus Basin. Our results suggest that there is a general increase in precipitation/ maximum and minimum temperature over the Upper Indus Basin/Lower Indus Basin by the end of the 21st century. It is also noted that the spatial variability of extreme climate indices is high during June to September (JJAS) than December to January (DJF). By the end of the century projections show that the precipitation changes are about 85% in JJAS and 40% in DJF with reference to the baseline (1995–2014) period over Indus Basin region. The temperature extreme indices are also increasing in future compare to the baseline period.

1. Introduction

An increased greenhouse gas concentration alters the radiation budget and thus the climate. Earth surface temperatures have shown a steady increase across the different regions of the globe and more significant precipitation variability. Recent Coupled Model Intercomparison Project (CMIP) models show climate change features under different emission pathways and provide the clue about the future climate with varying increments of temperatures. It is reported that among the many, the Indus river basin is also most vulnerable and very much prone to climate change (Immerzeel et al., 2020; Shreshta et al., 2019). Indus basin is characterized by a rapidly growing population with 250 million and having the highest cultivated lands in South Asia (e.g., Vinca et al., 2020). Changing rainfall and temperature projections will have a severe impact on the water availability over the Indus Basin and understanding these changes are essential for planning and managing water resources (e.g., Shreshta et al., 2019). Many studies reported the spatio-temporal variability of precipitation and temperature over the Indus Basin for different periods. Latif et al. (2018) studied the precipitation data obtained from the Pakistan Meteorological Department (PMD) over various Indus Basin locations. They found that decreasing and increasing trends of annual precipitation for the period of 1961 to 2013. Latif et al. (2020) analyzed the maximum and minimum temperature data sets from 1961 to 2013 obtained from the PMD. They reported the warming from the maximum temperature and mixed trends with the minimum temperature data sets over the Upper Indus River Basin. Minallah and Ivanov (2019) used the different precipitation data sets from ground truth, satellite, and reanalysis such as APHRODITE (1981–2007), GPCP (2001–2010), PERSIAN – CDR (2001–2010), TRMM (2001–2010), CMORPH-RAW (2001–2010), ERA-Interim (1981–2010), NCEP-CFSR (1981–2010) and GMFD (1981–2010) to report the connection of increasing frequency of ElNino to the interdecadal variability of rainfall over Indus basin. In-situ data of temperature showed an increase in maximum temperatures during winter and an increase in the diurnal temperature range in all seasons of

the year over the Indus Basin (e.g., Fowler and Archer, 2010). Many studies have documented pieces of evidence of historical climate change in the Indus basin. Among the observed trends in climatic variables, the increasing temperature trend is most consistent over the region.

Model simulations help the scientific community to study the future climate and its implications. Data of global and regional climate models provide an understanding in exploring the Indus Basin and various spatial and temporal scales. A few of the significant scientific outcomes of the research over Indus Basin (IB) using the models are i) higher precipitation over UIB than the LIB, ii) increase in future precipitation, iii) increase in extremes and iv) unprecedented warming. It is also reported that the IB is going to experience an increased frequency of extreme weather events in the future under different representative concentration pathways such as RCP4.5 & RCP8.5. Analysis of CMIP5 models suggests the uncertain water availability over UIB, leading to increased intensity and frequency of extreme discharges (Lutz et al., 2016). The increased rainfall and temperature projections over IB will affect the increased future flows and high snowmelt (Soncini et al., 2015). The possible changes in the precipitation and temperature characteristics in response to global warming will impact the hydrological regime-dependent socioeconomic of the basin, as noted by (e.g., Rajbhandari et al., 2015).

This study aims to investigate the impacts of climate change on the Indus Basin in the future the latest coupled model inter-comparison project phase 6 (CMIP6) projections. To this end, it is essential to obtain the future changes in the climate variables and their future extremes in response to global warming by using a high-resolution regional climate modeling system or downscaling of GCMs to a higher resolution. The advantage of downscaling and high-resolution regional climate simulations demonstrated the capability of capturing extreme precipitation events (Rao et al. 2014, Rao et al., 2020). However, studies on regional climate simulation for the extreme precipitation and temperature events are sparse. Future climate change will likely be associated with continued warming over the 21st century.

Given the above preamble, it is essential to understand the precipitation and temperature changes and their extreme behavior, which will help policymakers, design the proper framework mechanism under different climate change scenarios. The newly emerged statistically downscaled, bias-corrected, and high resolution (0.25° x 0.25°) data sets developed for South Asia by Mishra et al. (2020) from thirteen general circulation models (GCMs), under the CMIP6 have been used in the present study. Space and time scale variations of precipitation, maximum and minimum temperatures have been analyzed, and the extreme climate indices were obtained under different shared socioeconomic pathways (SSP) of SSP2-4.5 and SSP5-8.5 scenarios till the end of the 21st century. However, most of the earlier studies are focused on the different portions of the Indus basin. In contrast, minimal studies have been carried out on the precipitation and temperature changes and their extreme behavior in response to global warming in the future, covering the whole basin, which we will address in this paper.

2. Data And Analysis

The Indus River Basin is located between 72°E to 79°E longitude and 29°N to 37°N latitude. The Indus is one of the essential drainage systems of the subcontinent of India. It has a length of 2880 Km, of which 709Km lies in India. The catchment area of the Indus is about 1,165,000 Sq. Km, out of which about 321,248 Sq. Km is in India. This region was characterized by complex terrain and controlled by the Asian summer monsoon system and Western disturbances. The location map of the Indus river basin has given in the Fig. 1.

To account for climate change impacts in the Indus River Basin, we used the statistically downscaled, bias-corrected, and high resolution (0.25° x 0.25°) data sets developed for South Asia by Mishra et al. (2020a) from thirteen general circulation models (GCMs), under the coupled model inter-comparison project phase 6 (CMIP6), which are given in Table 1. Although some CMIP6 models have large ensemble members, they used a single member for each model for fair comparisons, typically the first ensemble member (r1i1p1f1 for CMIP6) to prepare the bias-corrected data.

The scenarios used in the CMIP6 are combined Shared Socioeconomic Pathways (SSP) and target radiative forcing levels at the end of the 21st century across two greenhouse gas emissions scenarios of SSP2-4.5 and SSP5-8.5. Daily precipitation, maximum and minimum temperature datasets generated by using Empirical Quantile Mapping (EQM) to statistically downscale over South Asia and Indian sub-continental river basins. More details for this are Empirical Quantile Mapping available at Mishra et al. (2020b). The historical run period is 1951 to 2014 for each experiment, and future projections from 2015 to 2100 forced with SSP2-4.5 (mid-range emissions) and SSP5-8.5 (high-end emissions) scenarios.

In this study, two primary observational datasets are used for the model validation. The model simulations are compared with high resolution gridded data sets prepared by APHRODITE (for precipitation) and Climate Prediction Center (CPC) for daily maximum and minimum air temperature available at 0.25° grid resolution for the period 1995–2014. For future climate projections, we used the three future time slices 2021–2040, 2051–2070, and 2081–2100, which are treated as a near (2030s), mid (2060s), and far future (2090s) under the two emission scenarios of SSP2-4.5 and SSP5-8.5. All the models used in the present study have been maintained to a uniform grid resolution for making them consistent with computing the multi-model mean. It will help the study to bring out the precise diagnosis of precipitation and temperature changes on a space and time scale.

The present study investigates the future changes in mean and extreme precipitation and temperature characteristics over the Indus basin in the near, mid, and far future with reference to the baseline period (1995–2014). We used seven key indices for precipitation and eight key indices for maximum and minimum temperatures defined by the ETCCDI (Zhang et al., 2011) for the present analysis. All the details for these indices are given in Table 2. All indices mentioned in this paper were calculated on a seasonal basis for the baseline and future scenarios of the 21st century, respectively.

Table 2
List of precipitation and temperature extreme indices used in this study

No.	Model Name	Coupled Model Name	Country	Key references
1	**ACCESS-CM2**	Australian Community Climate and Earth System Simulator-Climate Model 2	Australia	Dix et al. (2019)
2	**ACCESS-ESM1-5**	Australian Community Climate and Earth System Simulator-Earth System Model 1.5	Australia	Ziehn et al. (2020)
3	**BCC-CSM2-MR**	Beijing Climate Center, Climate System Model 2 (MR)	Wu et al. (2019)	
4	**CanESM5**	Canadian Earth System Model 5	Canada	Swart et al. (2019)
5	**EC-Earth3**	European Centre Earth Consortium model 3	Europe	EC-Earth, 2019a
6	**EC-Earth3-Veg**	European Centre Earth Consortium model 3 (Veg)	Europe	EC-Earth, 2019b
7	**INM-CM4-8**	Institute for Numerical Mathematics Climate Model 4.8	Russia	Volodin et al. (2018)
8	**INM-CM5-0**	Institute for Numerical Mathematics Climate Model 5	Russia	Volodin et al. (2018)
9	**MPI-ESM1-2-HR**	Max Planck Institute for Meteorology Earth System Model 1.2 (HR)	Germany	Gutjahr et al. (2019) Müller et al. (2018)
10	**MPI-ESM1-2-LR**	Max Planck Institute for Meteorology Earth System Model 1.2 (LR)	Germany	Mauritsen et al. (2019)
11	**MRI-ESM2-0**	Meteorological Research Institute Earth System Model 2.0	Japan	Yukimoto et al. (2019)
12	**NorESM2-LM**	Norwegian Earth System Model 2 (LM)	Norway	Seland et al. (2020)
13	**NorESM2-MM**	Norwegian Earth System Model 5 (MM)	Norway	Øyvind et al. (2020)

Table 3
CMIP6 models simulated seasonal mean precipitation is evaluated with APHRODITE observed data for the baseline period (1995–2014).

No.	Indices	Name	Definition	Units
Precipitation Indices				
1	RD	Rainy Day	A day with rainfall amount more than 2.5 mm	days
2	SDII	Simple daily intensity	The ratio of seasonal total precipitation to the number of wet days (≥ 1 mm)	mm/day
3	RX1DAY	Maximum 1-day precipitation	Seasonal maximum 1-day precipitation amount	mm
4	RX5DAY	Maximum consecutive 5-day precipitation	Seasonal maximum consecutive 5-day precipitation amount	mm
5	R10MM	Heavy precipitation days	Number of days with precipitation greater than 10 mm	days
6	R20MM	Very heavy precipitation days	Number of days with precipitation greater than 25 mm	days
7	CDD	Consecutive dry days	Seasonal maximum number of consecutive dry days (daily precipitation < 1 mm)	days
Temperature Indices				
1	Max_Tmax	Warmest day	Seasonal maximum value of daily max temperature	Deg.C
2	SU	Summer Days	Seasonal count of days when daily maximum temperature > 25°C	Days
3	CSU	Consecutive Summer Days	Seasonal largest number of consecutive summer days (maximum temperature > 25°C)	Days
4	ID	Ice Days	Seasonal count of days when daily maximum temperature < 0°C	Days

No.	Indices	Name	Definition	Units
5	Min_Tmin	Coldest Night	Seasonal minimum value of daily min temperature	Deg.C
6	FD	Frost Days	Seasonal count of days when daily minimum temperature < 0°C	Days
7	CFD	Consecutive Frost Days	Seasonal largest number of consecutive frost days (minimum temperature < 0°C)	Days
8	TR	Tropical Nights	Seasonal count of days when daily minimum temperature > 20°C	Days

Models	RMSE (mm/day)		Mean rainfall (mm/day)		S.D (mm/day)	
	JJAS	DJF	JJAS	DJF	JJAS	DJF
ACCESS-CM2	1.39	0.92	1.37	1.42	0.64	0.87
ACCESS-ESM1-5	1.62	0.91	1.60	1.01	0.58	0.61
BCC-CSM2-MR	0.75	0.67	2.03	1.16	0.91	0.56
CanESM5	2.01	1.40	0.54	1.88	0.47	1.04
EC-Earth3	0.77	0.49	2.00	1.04	0.83	0.59
EC-Earth3-Veg	0.77	0.48	2.09	0.89	0.90	0.62
INM-CM4-8	0.90	0.57	2.01	0.91	0.86	0.57
INM-CM5-0	1.03	0.93	1.47	1.38	0.67	0.82
MPI-ESM1-2-HR	1.10	0.58	1.52	1.11	0.55	0.90
MPI-ESM1-2-LR	1.01	0.76	1.69	1.31	0.76	0.82
MRI-ESM2-0	1.61	1.46	1.01	1.89	0.76	0.95
NorESM2-LM	1.68	1.59	0.87	2.07	0.93	1.10
NorESM2-MM	0.87	0.69	2.11	1.18	1.67	0.59

No.	Indices	Name	Definition	Units		
MMM	1.11	0.75	1.41	1.33	0.69	0.77
APHRODITE (OBS)	–	–	2.00	1.19	1.06	0.53

3. Results And Discussion

3.1 Evaluation of CMIP6 models simulated rainfall and temperature in the present climate

3.1.1 Rainfall

Figure 2. shows the mean annual cycle (in mm/day) over the Indus basin obtained from the individual GCMs of CMIP6 and their Multi-Model Mean (MMM) along with the observed APHRODITE data for the period 1995 to 2014. From the visual inspection, it was observed that all the models, along with their MMM and the observational data, captured the seasonal features reasonably well. By and large, the MMM could follow the pattern of APHRODITE in reliably showing the higher rainfall during the SW monsoon period with peak rain activity in July. CMIP6 MMM underestimated the rainfall during the SW monsoon season and overestimated it in the rest of months. Mean daily rainfall from CMIP6 MMM and APHRODITE varied from 1.25 mm and 0.75 mm in January, which is minimal during the year and from 2.1 mm to 2.5 mm during July. However, the CMIP6 models show distinguished variations in terms of magnitude, spread among models is high.

Figures.3 and 4 depict the spatial pattern of the summer monsoon (JJAS) and the winter season (DJF) mean daily rainfall over the Indus basin obtained from the thirteen CMIP6 GCM simulations along with their MMM and APHRODITE data sets. It is noted that the CMIP6 simulations showed very good skill in representing the present climate. Most of the models (except ACCESS-CM2, CanESM5, MRI-ESM2-0, and NorESM2-LM) and their MMM could show the higher rainfall region over the south-facing foothills of the Himalayas in summer, where the SW monsoon activity is higher than other areas. Rainfall is also higher over the upper Indus basin than the lower Indus basin, as depicted by the multi models and the observed data. During the winter season (Fig. 4), the upper Indus Basin experienced higher rainfall activity than the lower Indus basin. All the models and their MMM have reasonably well captured the winter rainfall (some of the models overestimated). Studies of Ali et al., (2015); Santosh and Shrestha (2015); Saeed et al., (2013) inferred that rainfall over UIB is high due to the influence of upper-level circulation over the mid-latitudes that connects the summer precipitation over the UIB. The spatial coverage of rainfall over the Indus Basin during SW monsoon and winter seasons shows a good agreement with the MMM and the APHRODITE data set.

Mean daily precipitation (mm/day), RMSE, and Standard Deviation provided in Table.3 for the Indus basin as a whole from the individual CMIP6 models, MMM, and APHRODITE data sets. The mean daily

rainfall is 2 mm and 1.19 mm for the IB during JJAS and DJF months obtained from the APHRODITE, whereas it is 1.41 and 1.33 mm from the CMIP6 MMM, respectively. Models such as ACCESS – ESM1-5, BCC-CSM2-MR, EC-Earth3, EC-Earth3 Veg, INM-CM4-8, INM-CM5-0, MP1-ESM1-2-HR, MP1-ESM1-2-LR, Nor ESM2 –NM showed the rainfall higher than the mean whereas the other models' ACCESS–CM2, Can ESM5, MRI-ESM2-0, Nor ESM2-LM show the lower rainfall than the MMM of CMIP 6 during the JJAS period. In winter, models such as ACCESS-CM2, CanESM5, INM-CM5-0, MRI-ESM2-0, and NorESM2-LM have shown rainfall values higher than the MMM. However, the models BCC-CSM2-MR, EC-Earth3, EC-Earth3–Veg, and INM-CM4-8 showed rainfall values of 2.03, 2.00, 2.09, 2.01mm/day, which are closer to that of the APHRODITE (2mm/day). Models BCC-CSM2-MR, MPI-ESM1-2-HR, and Nor ESM2 MM show the more comparable rainfall values of 1.16, 1.11, 1.18mm/day with the APHRODITE values (1.19 mm/day). The standard deviations of rainfall during the SW (winter) season for CMIP6 MMM and Aphrodite are 0.69 (0.77) and 1.06 (0.53), which infers the intermodal variability during the SW monsoon/winter season is lower/higher than the APHRODITE data sets.

Spatial variability of seven extreme precipitation indices viz RD, SDII, RX1DAY, RX5DAY, R10MM, R20MM, and CDD obtained from CMIP6 MMM and APHRODITE for the JJAS and DJF during baseline period (1995 to 2014) shown in Figs. 5 and 6. Most of the precipitation extreme indices are high over the UIB region except the CDD, which is higher over the LIB. Observed and MMM of CMIP6 show similar spatial variations. During the DJF period, the observed and CMIP6 MMM are in good agreement for most of the indices except in SDII. During JJAS the observations show higher spatial extent of a few indices such as R10MM, R20MM over the study region, which infers the underestimation in MMM compared to the observed in depicting the space scale variations of extreme indices. On the contrary, observed data sets are confined to the lesser region than MMM data sets to depict the R20MM extreme index over IB during the DJF period. The spatial variation in CDD is more conspicuous during the JJAS period than the DJF period, where they have varied up to 80 days and 60 days, respectively. The model results on spatial patterns are very similar to the observed pattern, but the model results show a higher/lower number of the precipitation extremes over the basin. However, over the high mountain regions, due to the terrain nature and the limitation in feasible model resolutions for simulating such areas, we conclude that the models performance is sufficient to analyze precipitation extremes.

3.1.2 Maximum and minimum temperature

The annual cycle of maximum and minimum temperatures over the IB is shown in Fig. 7 (a&b). The annual cycles for T_{max} and T_{min} are well simulated by the individual CMIP6 models and CMIP6 MMM with the highest temperatures in the monsoon months of June-July-August and the lowest temperatures in the winter months of December-January–February. The model simulated maximum and minimum temperatures are warmer than the observed temperatures. The maximum temperature crosses 30°C, and the minimum temperature goes as low as 2°C degrees. The model's spread low (which was significantly less), which means that individual model simulations are underestimated or overestimated. In contrast, the CMIP6 MMM is very close to the observations. However, the spread could be partly due to the

relatively high-resolution data chosen for representing the observed temperatures or the lack of observations in the mountain terrain in the Indus basin.

Daily maximum temperatures are considered for the month of June-July-August (JJA), being the hottest months for Indus Basin. Daily minimum temperatures are considered for December-January–February (DJF), being the coldest months. The mean seasonal maximum and minimum temperature patterns show the higher values over the LIB and lower values over UIB (Figs. 8 & 9). The MMM of CMIP6 shows a similar pattern obtained from the CPC data sets over the LIB compared to UIB. The LIB shows the temperature variations from 30 to above 40 spatially where the UIB goes beyond 35 degrees in both MMM and CPC data sets. It is reported that the warming over IB during the historical period of CMIP5 (1979–2005) show higher uncertainties than over the future epochs when compared with the framework of the coordinated regional climate downscaling experiment for South Asia (CX-SA) (Hasson et al., 2019). Pomee and Hertig (2021) reported the excellent agreement of GCMs of CMIP5 with the ERM – Interim maximum and minimum temperatures over different parts of the Indus Basin in Pakistan. The CMIP6 MMM simulations show reasonable skill in representing the spatial patterns of temperatures over the Indus Basin.

Temperature extremes are generally characterized by the frequency and intensity of daily temperatures exceeding certain tolerable limits. For extreme temperature indices, the spatial climatology patterns compared between CPC and, the CMIP6 MMM are shown in Figs. 10 & 11. The highest daily maximum temperature days, SU days and CSU days, and ID are higher than 40, 90, and 85 days from June to August, as depicted by CMIP6 MMM and CPC. The CMIP6 MMM and observed indices are well in agreement over LIB in these categories except over a few portions of UIB. ID has shown considerable variations from CMIP6 MMM to observed, particularly over the UIB, which needs further studies to understand these changes by causal factors. Similar features observed in China and the studies of (Wang et al. 20140 reported due to complex terrain, the characteristics of ID in China may be due to the intense moisture transport, Asian low, etc. However, over the UIB, the observed data sets could not show SU and CSU days, where the MMM show considerable variation up to nine days. Overall, the CMIP6 MMM can generally reproduce the CPC mean spatial climatology pattern for these maximum temperature extremes reasonably well (Fig. 10).

The UIB has shown less number of lowest minimum temperature days with the observed data sets while the CMIP6 MMM depicts the little higher minimum temperature days. The other extreme indices, such as FD and CFD, had some differences in capturing similar MMM variations and observed data sets. The FD and CFD over UIB have increased beyond 70 days and as low as ten days in the LIB region. Tropical nights (TR) are more than seven days over the LIB and less than over UIB (Fig. 11). The studies of Yaseen et al. (2020) reported a spatiotemporal variation in temperature trends over the UIB. As UIB consists of Shyok and Shigar, Astore and Haunza, Gilgit, Jehlum, and Kabul sub-basin as part of UIB, which have different elevations, regions with low altitude face the warming trend, and the areas with high altitude show the cooling trends. Hence, we may also expect the variations among the extremes of the temperature over the UIB with models and observed data. As the historical study periods show warming

and cooling over the Indus basin, future temperature extreme trends play a crucial role in understanding the IB climate. It is also clear that the multi-model mean is generally more skillful than the individual models for extreme temperature indices.

3.2 Projected changes

3.2.1 Seasonal mean rainfall and its extreme indices

The main focus of the work is to see the aforementioned extreme precipitation indices in future climate scenarios. For this purpose, we have obtained the precipitation changes with reference to the baseline over IB during near (2030s), mid (2060s) of the century, and far (2090s) future of the 21st century under the shared socioeconomic pathways of SSP-24.5 & SSP-5 8.5 scenarios for JJAS and DJF seasons. By visual inspection, Fig. 12 provides a basic understanding of the rainfall to increase under the IB climate change scenario. Many studies reported that the rainfall, particularly over UIB, is projected to increase under different climate change scenarios when used the CMIP5 data sets. Studies of Rajbhandari et al., (2015) on the projected changes of climate over IB using the PRECIS model revealed the projected rainfall over UIB, LIB, and border areas will increase, decrease and change very little respectively during the different epochs of the 21st century. Dimri et al., (2018) also reported the increase/decrease in future rainfall over UIB/LIB under different representative concentration pathways. They found a strong linkage of water budget to the corresponding precipitation changes over the Indus Basin. The present analysis shows that the projection of an increase in rainfall is higher during the JJAS period than in the DJF period, with a lower/higher increase during SSP2-4.5 and SSP5-8.5 emission scenarios. The histograms in Fig. 12 clearly shows that the CMIP6 MMM in JJAS rainfall is likely to increase from the near to far future (around 30 to 60% under SSP2- 4.5 and 45 to 85% under SSP5-8.5), whereas in DJF, the rainfall may increase (around 5 to 15% under SSP2-4.5 and 5 to 35% under SSP5-8.5). Almazroui et al. (2020) revealed the increase of annual precipitation obtained from CMIP6 is about 49.1% over Bangladesh, 160.5% over India, and 159.7% over Pakistan by the end of the century. Studies revealed that the precipitation obtained from the CMIP6 models show a continuous increase compared to that of in CMIP5 models over different parts of the world, South Asian countries, particularly Zhu et al., (2020); Almazroui et al., (2020). Studies also show that CMIP6 has better skills in representing the rainfall than CMIP5 over Asia's regions (Chen et al., 2021), India (Katzenberger et al., 2021). Therefore, it is evident that the increase in precipitation is observed in both seasons under different emission scenarios (SSP2-4.5 & SSP5-8.5). Higher monsoon precipitation with sub-stantial changes are projected by the late 21st century with increasing GHGs under SSP2-4.5 & SSP5-8.5 scenarios. The enhanced thermodynamic conditions due to global warming may result in the increase of seasonal precipitation.

Figure 13 & 14 shows the future changes in the precipitation extremes during the JJAS season under SSP2-4.5 and SSP5-8.5 emission scenarios obtained from the CMIP6 models. The extreme indices show a perceptible increase during the different future epochs with distinguished variations. Event-based precipitation indices such as R10MM, R20MM show higher variability than the other indices. It is also worth noting that the variation is more during the SSP2-4.5 scenario than the SSP5-8.5 scenario. The CDD

increased under the SSP2-4.5 scenario compared to the SSP5-8.5 scenario. During the mid-future (2060s), the CDD could show fewer variations than the near-future (2030s) in the SSP2-4.5 scenario, whereas it continuously decreased during the SSP5-8.5 scenario. Studies of Siddique et al., (2020) used the ensemble of three GCMs for CMIP5 and reported the extreme precipitation projections. They found that an increase in very wet days and heavy precipitation days in the future over the Jhelum river basin, which is part of the Indus river basin. Dahri et al., (2021) used the ensemble of CMIP5, and they identified different trends of rainfall in the future that is varied spatially over the Indus basin and reported the intensification of the hydrological regime over the Indus Basin. Our spatial analyses of extreme precipitation indices show the variation over IB with higher values over UIB while the lower ones over LIB. The extreme climate indices RD, SDII, RX1DAY, RX5DAY, R10MM and R20MM has an increased percentage with a maximum of 89%, 39%, 71%, 89%, 95%, and 95% during SSP5-8.5scenario. The rising temperature might lead to increased snow and ice melting, which could increase the intensity and frequency of extreme precipitation events in the future. The extreme precipitation indices obtained during DJF season over IB also showed the increased projections under different future emission scenarios (not shown in Figure). The projections in precipitation indices show the overall increase of the extreme events over the Indus basin in the future due to enhanced levels of GHGs. In summary, a robust rise in seasonal precipitation extremes between the present climate and future climate can be derived under global warming.

3.2.2 Seasonal mean maximum and minimum temperature and its extreme indices

Like precipitation changes, the maximum and minimum temperatures show monotonous increase towards the end of the 21st century over the Indus basin shown in Figs. 15 & 16. These features are seen in all three epochs. Figures 15 & 16 infer the drastic rise in maximum temperature/minimum temperature over UIB/LIB during the future epochs under both SSP2-4.5 & SSP5-8.5 scenarios. A rise in 6^0C in maximum temperature is witnessed with an area experienced by these changes that considerably extended during JJA in both scenarios. In general, SSP5-8.5 scenario has shown more changes compared to SSP2-4.5 scenario. Spatial maps of minimum temperature over IB show that the entire basin is more vulnerable to minimum temperature changes by the end of the 21st century. CMIP6 MMM simulations for the 2030s, 2060s, and 2090s indicate all-around warming over the Indus basin associated with increasing greenhouse gas concentrations. Studies by (Pepin and Lundquist 2008; Pepin et al., 2015; Sabin et al., 2020) found that most of the climate models consistently show enhanced warming in the mountainous region than found in observations, and also they identified that mountain temperatures are increasing at a faster rate than the global average.

Figures 17 & 18 show the percentage change in temperature extremes during the 2030s, 2060s, and 2090s. From the figures, it can be understood that the percentage of temperature extremes gradually increased from the 2030s to the 2090s. A drastic variation from 75–90% is observed in the category of consecutive summer days; in contrast, the variation is lowest in ice days when the extremes related to maximum temperature are considered during SSP 5-8.5 scenarios. In minimum temperature extremes,

tropical nights have undergone highest change under the SSP5-8.5 scenario, whereas it is the lowest in the minimum temperature days category. Similar results are noted over the UIB when the analysis is carried out with CMIP5 data sets by (Saddique et al., 2020), where they have reported the increasing trends of the frequency of warm days, summer days, and warm nights, etc. An analysis on the Hind Kush region using CMIP5 models under RCP4.5 & 8.5 scenarios revealed the general increase in temperature with the highest during 2066–2099 and the increase in temperature extremes (Wu et al., 2017). This comprehensive study shows that the increase in precipitation and warming over Indus Basin and may have a significant impact on the hydrology of the Indus Basin in terms of flows (Khan et al., 2020, discharge (Wijngaard et al., 2017) and water budget (Dimri et al., 2018). The results indicate considerable change in these extreme indices by the end of twenty-first century over Indus basin, which is very well supported by the latest CMIP version models.

4. Conclusions

Climate change is one of the major threats to the water budget of the Indus Basin. In view of this, our study aimed to focus on the spatiotemporal variations of precipitation and maximum and minimum temperatures during the present and future climate in response to global warming by using the statistically downscaled bias-corrected climate model projections under different socioeconomic pathways proposed in the suite of CMIP6 models. In this study, the outputs from thirteen downscaled models have been analyzed to examine the fidelity of models in simulating the observed pattern and extreme indices characteristics indices over the Indus basin. The CMIP6 MMM is compared with the observed data sets such as APHRODITE (for precipitation), CPC (for maximum and minimum temperatures) for the historical/baseline period 1995 to 2014. Further, we also presented the changes in future precipitation and temperature extremes over the Indus Basin.

This study reports that i) a general agreement of MMM of CMIP 6 with the observed data sets with high variations in UIB, ii) all the rainfall extremes show higher values over the UIB while CDD has shown a higher number of days over LIB during JJAS and DJF seasons, iii) the projected precipitation shows increasing trend during the future epochs with highest being depicted during the 2090s with change approximately 40% to the baseline period, iv) UIB/LIB experienced a higher number of maximum/minimum temperature extremes during JJAS/DJF seasons of 1979 to 2014, v) maximum/minimum temperature changes in percentage are high during SSP5-8.5 scenario compared to SSP2-4.5 scenario with maximum change (up to 6%) observed during the 2090s of the 21st century and vi) summer days show more than 75% high from the baseline during JJAS, while the TR showed the highest (> 60%) during DJF season in all future epochs. The results obtained from newly available CMIP6 future projections confirm the changes in precipitation and temperature over the Indus Basin region.

Declarations

Acknowledgments

The authors are grateful to the newly emerged statistically downscaled, bias-corrected, and high-resolution CMIP6 data for Indus Basin and making such data available to carry out the present study. The authors are also grateful to the APHRODITE data providers for sharing their gridded precipitation data sets. Thanks to *CPC Global Temperature data provided by the NOAA/OAR/ESRL PSL.*

References

Ali, S.; Li, D.; Congbin, F.; Khan, F. 2015. Twenty first century climatic and hydrological changes over Upper Indus Basin of Himalayan region of Pakistan. *Environ. Res. Lett.10*, 14007.

Almazroui, M., Saeed, S., Saeed, F. *et al.* Projections of Precipitation and Temperature over the South Asian Countries in CMIP6. 2020. *Earth Syst Environ* **4,** 297–320, https://doi.org/10.1007/s41748-020-00157-7.

Chao-An Chen, Huang-Hsiung Hsu, Hsin-Chien Liang. 2021. Evaluation and comparison of CMIP6 and CMIP5 model performance in simulating the seasonal extreme precipitation in the Western North Pacific and East Asia,Weather and Climate Extremes,Volume 31,100303,ISSN 2212-0947,https://doi.org/10.1016/j.wace.2021.100303

Dahri ZH, Ludwig F, Moors E, Ahmad S, Ahmad B, Ahmad S, Riaz M, Kabat P.2021. Climate change and hydrological regime of the high-altitude Indus basin under extreme climate scenarios. Sci Total Environ., 2;768:144467. doi: 10.1016/j.scitotenv.2020.144467.

Dimri, A.P.; Kumar, D.; Chopra, S.; Choudhary, A. 2019. Indus River Basin: Future climate and water budget. Int. J. Climatol. 39, 395–406.

Dix, M., Bi, D., Dobrohotoff, P., Fiedler, R., Harman, I., Law, R., & Yang, R. 2019. CSIRO-ARCCSS ACCESS-CM2 model output prepared for CMIP6 CMIP historical. Earth System Grid Federation. https://doi.org/10.22033/ESGF/CMIP6.4271.

EC-Earth, 2019a. EC-Earth-Consortium EC-Earth3 model output prepared for CMIP6 CMIP historical. https://doi.org/10.22033/ESGF/CMIP6.4700.

EC-Earth, 2019b. EC-Earth-Consortium EC-Earth3-Veg model output prepared for CMIP6 CMIP historical. https://doi.org/10.22033/ESGF/CMIP6.4706.

Fowler H J, Archer D R. 2010. Conflicting signals of climatic change in the Upper Indus Basin. Journal of Climate, 19(17): 4276–4293.

Gutjahr O, Putrasahan D, Lohmann K, Jungclaus JH, von Storch J-S, Brüggemann N, Haak H, Stössel A. 2019. Max Planck Institute Earth System Model (MPI-ESM1.2) for the High-Resolution Model Intercomparison Project (HighResMIP). Geosci Model Dev 12:3241–3281. https://doi.org/10.5194/gmd-12-3241-2019

Hasson, S., Böhner, J. & Chishtie, F. 2019. Low fidelity of CORDEX and their driving experiments indicates future climatic uncertainty over Himalayan watersheds of Indus basin. *Clim Dyn* **52,** 777–798. https://doi.org/10.1007/s00382-018-4160-0

Immerzeel, W.W., Lutz, A.F., Andrade, M. *et al.* 2020. Importance and vulnerability of the world's water towers. *Nature* **577,** 364–369. https://doi.org/10.1038/s41586-019-1822-y

Katzenberger, A., Schewe, J., Pongratz, J., and Levermann, A. 2021. Robust increase of Indian monsoon rainfall and its variability under future warming in CMIP-6 models, Earth Syst. Dynam. Discuss. [preprint], https://doi.org/10.5194/esd-2020-80.

Khan, A.J.; Koch, M.; Tahir, A.A. 2020. Impacts of Climate Change on the Water Availability, Seasonality and Extremes in the Upper Indus Basin (UIB). *Sustainability*, *12*, 1283. https://doi.org/10.3390/su12041283.

Latif, Y., Yaoming, M. & Yaseen, M. 2018. Spatial analysis of precipitation time series over the Upper Indus Basin. *Theor Appl Climatol* **131,** 761–775, https://doi.org/10.1007/s00704-016-2007-3

Latif, Y., Yaoming, M., Yaseen, M. *et al.* 2020. Spatial analysis of temperature time series over the Upper Indus Basin (UIB) Pakistan. *Theor Appl Climatol* **139,** 741–758https://doi.org/10.1007/s00704-019-02993-8

Lin, L., Wang, Z., Xu, Y., Fu, Q., & Dong, W. 2018. Larger sensitivity of precipitation extremes to aerosol than greenhouse gas forcing in CMIP5 models. Journal of Geophysical Research: Atmospheres, 123, 8062–8073. https://doi.org/10.1029/ 2018JD028821

Lutz AF, Immerzeel WW, Kraaijenbrink PDA, Shrestha AB, Bierkens MFP. 2016. Climate Change Impacts on the Upper Indus Hydrology: Sources, Shifts and Extremes. PLoS ONE 11(11): e0165630. https://doi.org/10.1371/journal.pone.0165630

Mauritsen T, Bader J, Becker T, Behrens J, Bittner M, Brokopf R et al. 2019. Developments in the MPI-M Earth System Model version 1.2 (MPI-ESM1.2) and its response to increasing CO2. J Adv Model Earth Syst 11:998–1038. https://doi.org/10.1029/2018M S001400

Minallah, S.; Ivanov, V.Y. 2019. Interannual variability and seasonality of precipitation in the Indus River basin. J. Hydrometeorol. 20, 379–395.

Mishra, V., Bhatia, U. & Tiwari, A.D. 2020a. Bias-corrected climate projections for South Asia from Coupled Model Intercomparison Project-6. *Sci Data* **7,** 338. https://doi.org/10.1038/s41597-020-00681-1

Mishra, V., Bhatia, U. & Tiwari, A. D. 2020b. Bias corrected climate projections from CMIP6 models for Indian sub-continental river basins. *Zenodo* https://doi.org/10.5281/zenodo.3874046.

Pepin N and Lundquist J .2008. Temperature trends at high elevations: Patterns across the globe; Geophys. Res. Lett. 35 1–L14701.

Pepin N et al. 2015. Elevation-dependent warming in mountain regions of the world; Nat. Clim. Change 5 424–430.

Pomee, M.S.; Hertig, E. 2021. Temperature Projections over the Indus River Basin of Pakistan Using Statistical Downscaling. Atmosphere, 12, 195. https://doi.org/ 10.3390/atmos12020195.

Rajbhandari, R., Shrestha, A.B., Kulkarni, A. *et al.2015.* Projected changes in climate over the Indus river basin using a high resolution regional climate model (PRECIS). *Clim Dyn* **44,** 339–357. https://doi.org/10.1007/s00382-014-2183-8

Rao KK, Patwardhan SK, Kulkarni A, Kamala K, Sabade SS, Kumar KK .2014. Projected changes in mean and extreme precipitation indices over India using PRECIS. Glob Planet Chang 113:77–90

Rao, K.K., Kulkarni, A., Patwardhan, S. et al. 2020. Future changes in precipitation extremes during northeast monsoon over south peninsular India. *Theor Appl Climatol* **142,** 205–217. https://doi.org/10.1007/s00704-020-03308-y

Sabin T P et al. 2020. Climate change over the Himalayas; In: Assessment of Climate Change over the Indian Region (eds) Krishnan R, Sanjay J, Gnanaseelan C, Mujumdar M, Kulkarni A and Chakraborty S, Springer, Singapore, https:// doi.org/10.1007/978-981-15-4327-2˙11.

Saddique, N., Khaliq, A. & Bernhofer, C.2020. Trends in temperature and precipitation extremes in historical (1961–1990) and projected (2061–2090) periods in a data scarce mountain basin, northern Pakistan. *Stoch Environ Res Risk Assess* **34,** 1441–1455. https://doi.org/10.1007/s00477-020-01829-6

Saeed, F., Hagemann, S., Saeed, S. et al. 2013. Influence of mid-latitude circulation on upper Indus basin precipitation: the explicit role of irrigation. *Clim Dyn* **40,** 21–38 (2013). https://doi.org/10.1007/s00382-012-1480-3

Santosh Nepal & Arun Bhakta Shrestha .2015. Impact of climate change on the hydrological regime of the Indus, Ganges and Brahmaputra river basins: a review of the literature, International Journal of Water Resources Development, 31:2, 201-218, DOI: 10.1080/07900627.2015.1030494

Seland Ø, Bentsen M, Seland Graf L, Olivié D, Toniazzo T, Gjermundsen A, Debernard JB, Gupta AK, He Y, Kirkevåg A, Schwinger J, Tjiputra J, Schancke Aas K, Bethke I, Fan Y, Griesfeller J, Grini A, Guo C, Ilicak M, Hafsahl Karset IH, Landgren O, Liakka J, Onsum Moseid K, Nummelin A, Spensberger C, Tang H, Zhang Z, Heinze C, Iverson T, Schulz M. 2020. The Norwegian Earth System Model, NorESM2—Evaluation of theCMIP6 DECK and historical simulations. Geosci Model Dev Discuss.

Shrestha A B, Nisha Wagla and Rajbhandari R .2019. A review on the projected changes in climate over the Indus Basin; In: *Indus River Basin: Water Security and Sustainability* (eds) Khan S I and Adams T E.

Elsevier, pp. 145–157, https://doi.org/10.1016/B978-0-12-812782-7.00007-2.

Soncini, A.; Bocchiola, D.; Confortola, G.; Bianchi, A.; Rosso, R.; Mayer, C.; Lambrecht, A.; Palazzi, E.; Smiraglia, C.; Diolaiuti, G. 2015. Future hydrological regimes in the upper indus basin: A case study from a high-altitude glacierized catchment. *J. Hydrometeorol.16*, 306–326.

Swart NC, Cole JNS, Kharin VV, Lazare M, Scinocca JF, Gillett NP, Anstey J, Arora V, Christian JR, Hanna S, Jiao Y, Lee WG, Majaess F, Saenko OA, Seiler C, Seinen C, Shao A, Sigmond M, Solheim L, von Salzen K, Yang D, Winter B. 2019. The Canadian Earth System Model version 5 (CanESM5.0.3). Geosci Model Dev 12:4823–4873. https://doi.org/10.5194/gmd-12-4823-2019

Volodin EM, Mortikov EV, Kostrykin SV, Galin VYa, Lykossov VN, Gritsun AS, Diansky NA, Gusev AV, Iakovlev NG, Shestakova AA, Emelina SV. 2018. Simulation of the modern climate using the INM-CM48 climate model. Russ J Numer Anal Math Model 33(6):367–374. https://doi.org/10.1515/rnam-2018-0032

Volodin, Evgeny; Mortikov, Evgeny; Gritsun, Andrey; Lykossov, Vasily; Galin, Vener; Diansky, Nikolay; Gusev, Anatoly; Kostrykin, Sergey; Iakovlev, Nikolay; Shestakova, Anna; Emelina, Svetlana**. 2019**. *INM INM-CM5-0 model output prepared for CMIP6 CMIP piControl*. Version *YYYYMMDD*[1].Earth System Grid Federation. https://doi.org/10.22033/ESGF/CMIP6.5081

Vinca, A., Parkinson, S., Riahi, K. et al. 2020. Transboundary cooperation a potential route to sustainable development in the Indus basin. *Nat Sustain.* https://doi.org/10.1038/s41893-020-00654-7

Wang, Z. Y., S. Yang, Z. J. Ke, and X. W. Jiang. 2014. Large-scale Atmospheric and Oceanic Conditions for Extensive and Persistent Icing Events in China. Journal of Applied Meteorology and Climatology 53 (12): 2698–2709. doi:10.1175/JAMC-D-14-0062.1.

Wijngaard RR, Lutz AF, Nepal S, Khanal S, Pradhananga S, Shrestha AB, et al. 2017. Future changes in hydro-climatic extremes in the Upper Indus, Ganges, and Brahmaputra River basins. PLoS ONE 12(12): e0190224. https://doi.org/10.1371/journal.pone.0190224

Wu T, Lu Y, Fang Y, Xin X, Li L, Li W, Jie W, Zhang J, Liu Y, Zhang L, Zhang F, Zhang Y, Wu F, Li J, Chu M, Wang Z, Shi X, Liu X, Wei M, Huang A, Zhang Y, Liu X. 2019. The Beijing Climate Center Climate System Model (BCC-CSM): the main progress from CMIP5 to CMIP6. Geosci Model Dev 12:1573–1600. https ://doi.org/10.5194/gmd-12-1573-2019

Wu J, Xu Y, Gao XJ. 2017. Projected changes in mean and extreme climates over Hindu Kush Himalayan region by 21 CMIP5 models. Adv Clim Chang Res 8(3):176–184. https://doi.org/10.1016/j.accre.2017.03.001

Yaseen, M.; Ahmad, I.; Guo, J.; Azam, M.I.; Latif, Y. 2020. Spatiotemporal Variability in the Hydrometeorological Time-Series over Upper Indus River Basin of Pakistan. Adv. Meteorol. 5852760, doi:10.1155/2020/5852760

Yukimoto S, Kawai H, Koshiro T, Oshima N, Yoshida K, Urakawa S, Tsujino H, Deushi M, Tanaka T, Hosaka M, Yabu S, Yoshimura H, Shindo E, Mizuta R, Obata A, Adachi Y, Ishii M . 2019. The Meteorological Research Institute Earth System Model version 2.0, MRI-ESM2.0: description and basic evaluation of the physical component. J Meteorol Soc Jpn. https://doi.org/10.2151/jmsj.2019-051

Zhang, X., Alexander, L., Hegerl, G.C., Jones, P., Klein Tank, A., Peterson, T.C., Trewin, B., Zwiers, F.W. 2011. Indices for monitoring changes in extremes based on daily temperature and precipitation data. WIREs Clim. Chang. 2, 851–870.

Zhu Y, Yang S. 2020. Evaluation of CMIP6 for historical temperature and precipitation over the Tibetan plateau and its comparison with CMIP5. *Advances in Climate Change Research* 11: 239–251. https://doi.org/10.1016/j.accre.2020.08.001

Tables

Information of 13 CMIP6 climate models

Model Name	Coupled Model Name	Country	Key references
ACCESS-CM2	Australian Community Climate and Earth System Simulator-Climate Model 2	Australia	Dix et al. (2019)
ACCESS-ESM1-5	Australian Community Climate and Earth System Simulator-Earth System Model 1.5	Australia	Ziehn et al. (2020)
BCC-CSM2-MR	Beijing Climate Center, Climate System Model 2 (MR)	China	Wu et al. (2019)
CanESM5	Canadian Earth System Model 5	Canada	Swart et al. (2019)
EC-Earth3	European Centre Earth Consortium model 3	Europe	EC-Earth, 2019a
EC-Earth3-Veg	European Centre Earth Consortium model 3 (Veg)	Europe	EC-Earth, 2019b
INM-CM4-8	Institute for Numerical Mathematics Climate Model 4.8	Russia	Volodin et al. (2018)
INM-CM5-0	Institute for Numerical Mathematics Climate Model 5	Russia	Volodin et al. (2018)
MPI-ESM1-2-HR	Max Planck Institute for Meteorology Earth System Model 1.2 (HR)	Germany	Gutjahr et al. (2019) Müller et al. (2018)
MPI-ESM1-2-LR	Max Planck Institute for Meteorology Earth System Model 1.2 (LR)	Germany	Mauritsen et al. (2019)
MRI-ESM2-0	Meteorological Research Institute Earth System Model 2.0	Japan	Yukimoto et al. (2019)
NorESM2-LM	Norwegian Earth System Model 2 (LM)	Norway	Seland et al. (2020)
NorESM2-MM	Norwegian Earth System Model 5 (MM)	Norway	Øyvind et al. (2020)

List of precipitation and temperature extreme indices used in this study

Indices	Name	Definition	Units
Precipitation Indices			
D	Rainy Day	A day with rainfall amount more than 2.5 mm	days
DII	Simple daily intensity	The ratio of seasonal total precipitation to the number of wet days (≥ 1 mm)	mm/day
X1DAY	Maximum 1-day precipitation	Seasonal maximum 1-day precipitation amount	mm
X5DAY	Maximum consecutive 5-day precipitation	Seasonal maximum consecutive 5-day precipitation amount	mm
10MM	Heavy precipitation days	Number of days with precipitation greater than 10 mm	days
20MM	Very heavy precipitation days	Number of days with precipitation greater than 25 mm	days
DD	Consecutive dry days	Seasonal maximum number of consecutive dry days (daily precipitation < 1 mm)	days
Temperature Indices			
lax_Tmax	Warmest day	Seasonal maximum value of daily max temperature	Deg.C
U	Summer Days	Seasonal count of days when daily maximum temperature >25°C	Days
SU	Consecutive Summer Days	Seasonal largest number of consecutive summer days (maximum temperature >25°C)	Days
D	Ice Days	Seasonal count of days when daily maximum temperature <0°C	Days
lin_Tmin	Coldest Night	Seasonal minimum value of daily min temperature	Deg.C
D	Frost Days	Seasonal count of days when daily minimum temperature <0°C	Days
FD	Consecutive Frost Days	Seasonal largest number of consecutive frost days (minimum temperature <0°C)	Days
R	Tropical Nights	Seasonal count of days when daily minimum temperature >20°C	Days

Table 3. CMIP6 models simulated seasonal mean precipitation is evaluated with APHRODITE observed data for the baseline period (1995-2014).

Models	RMSE (mm/day)		Mean rainfall (mm/day)		S.D (mm/day)	
	JJAS	DJF	JJAS	DJF	JJAS	DJF
ACCESS-CM2	1.39	0.92	1.37	1.42	0.64	0.87
ACCESS-ESM1-5	1.62	0.91	1.60	1.01	0.58	0.61
BCC-CSM2-MR	0.75	0.67	2.03	1.16	0.91	0.56
CanESM5	2.01	1.40	0.54	1.88	0.47	1.04
EC-Earth3	0.77	0.49	2.00	1.04	0.83	0.59
EC-Earth3-Veg	0.77	0.48	2.09	0.89	0.90	0.62
INM-CM4-8	0.90	0.57	2.01	0.91	0.86	0.57
INM-CM5-0	1.03	0.93	1.47	1.38	0.67	0.82
MPI-ESM1-2-HR	1.10	0.58	1.52	1.11	0.55	0.90
MPI-ESM1-2-LR	1.01	0.76	1.69	1.31	0.76	0.82
MRI-ESM2-0	1.61	1.46	1.01	1.89	0.76	0.95
NorESM2-LM	1.68	1.59	0.87	2.07	0.93	1.10
NorESM2-MM	0.87	0.69	2.11	1.18	1.67	0.59
MMM	1.11	0.75	1.41	1.33	0.69	0.77
APHRODITE (OBS)	--	--	2.00	1.19	1.06	0.53

Figures

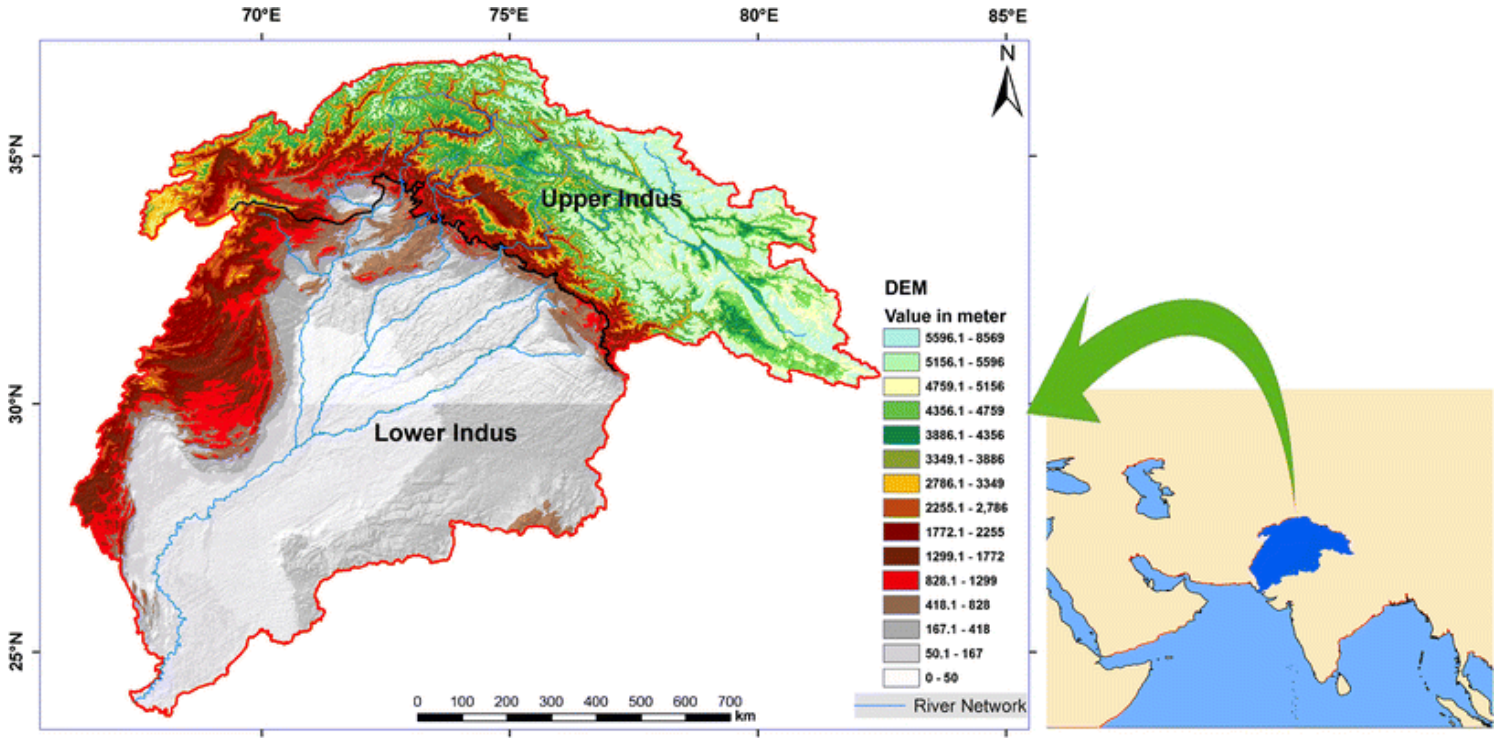

Figure 1

Location map of the Indus river basin (Rajbhandari et al., 2015)

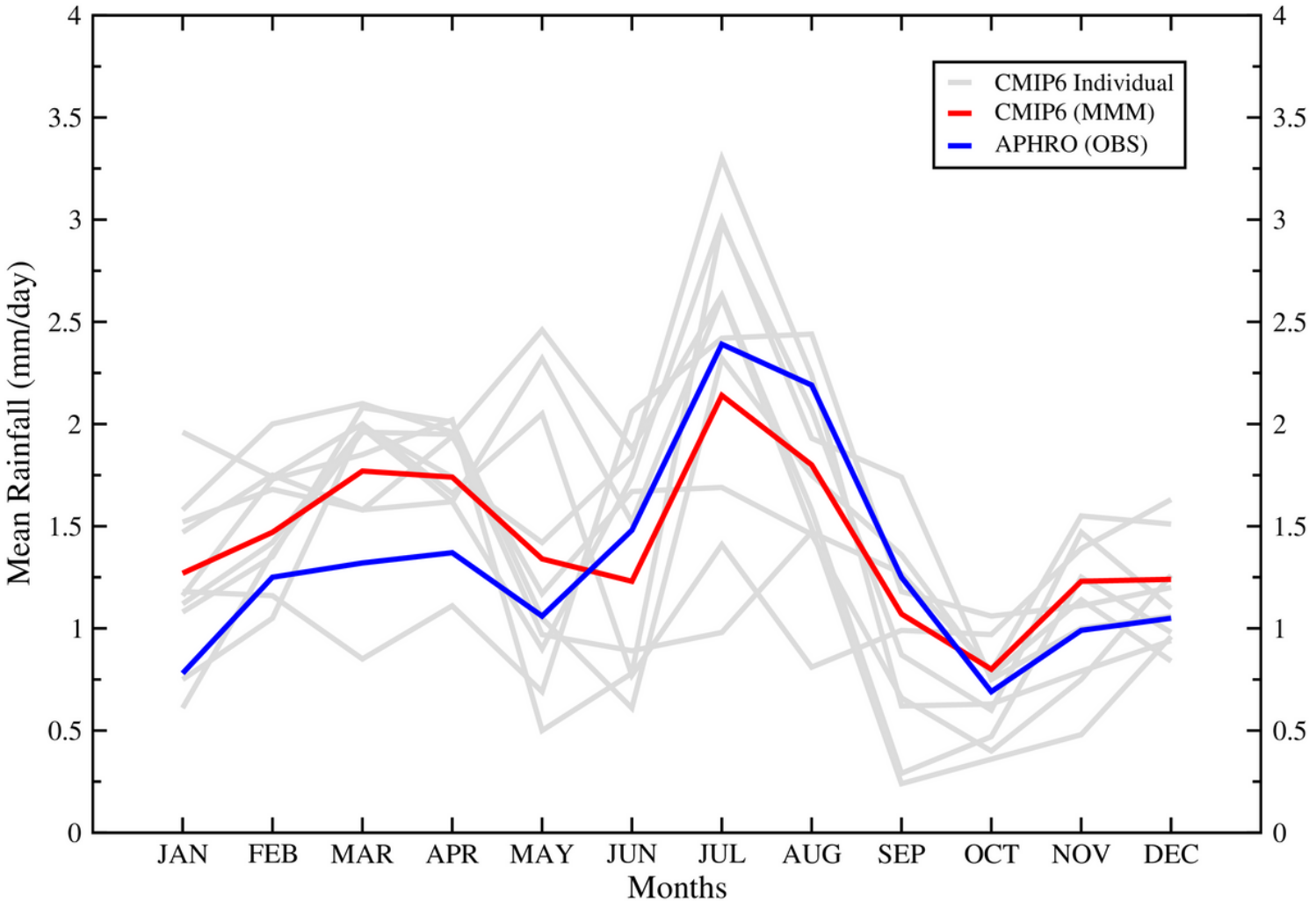

Figure 2

Annual cycles of mean precipitation over the Indus basin from the CMIP6 models compared with APHRODITE precipitation data during the baseline period (1995–2014).

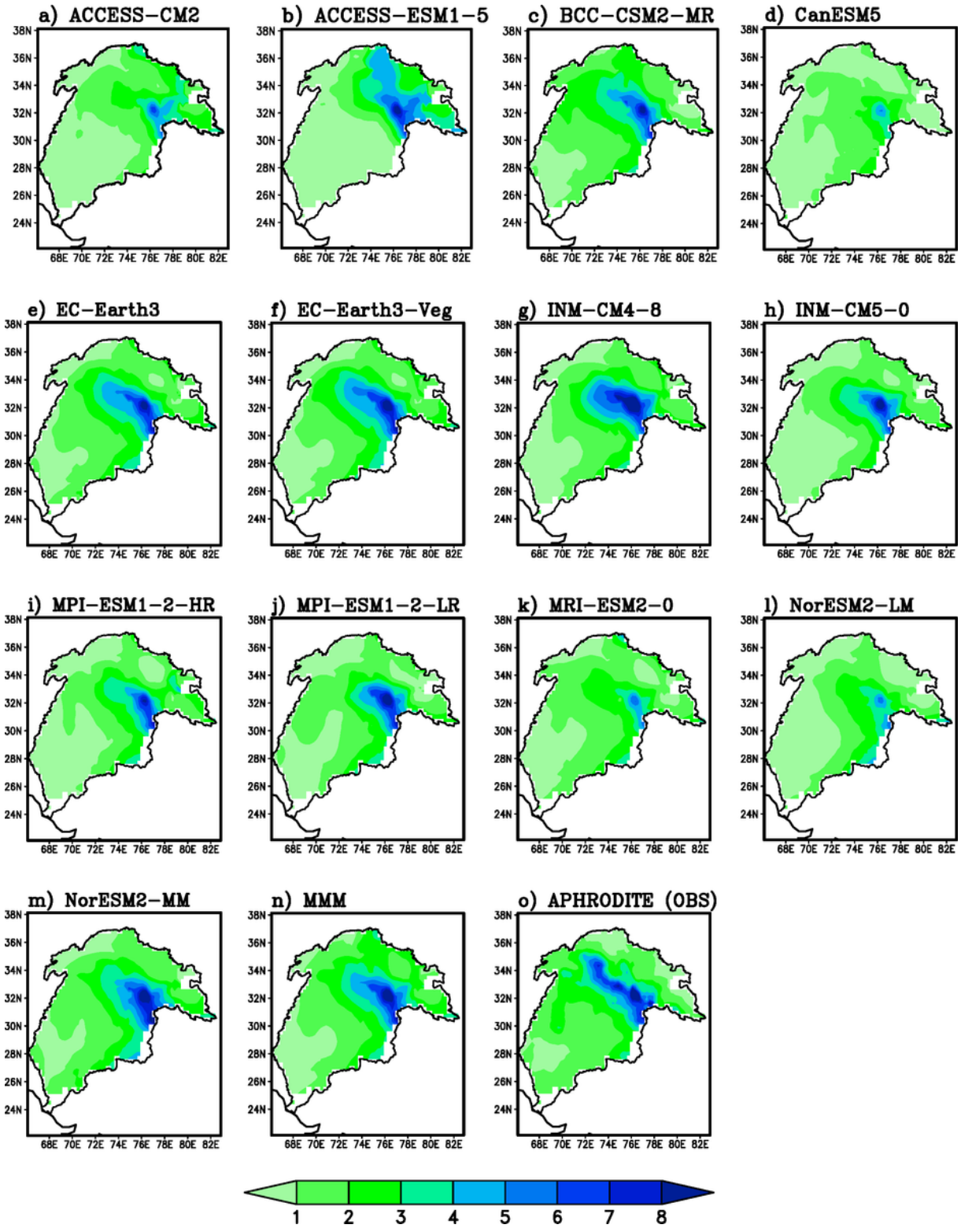

Figure 3

Spatial distribution of the summer monsoon (JJAS) rainfall (mm/day) as captured by CMIP6 individual models and their MMM compared with the APHRODITE for the baseline period (1995–2014)

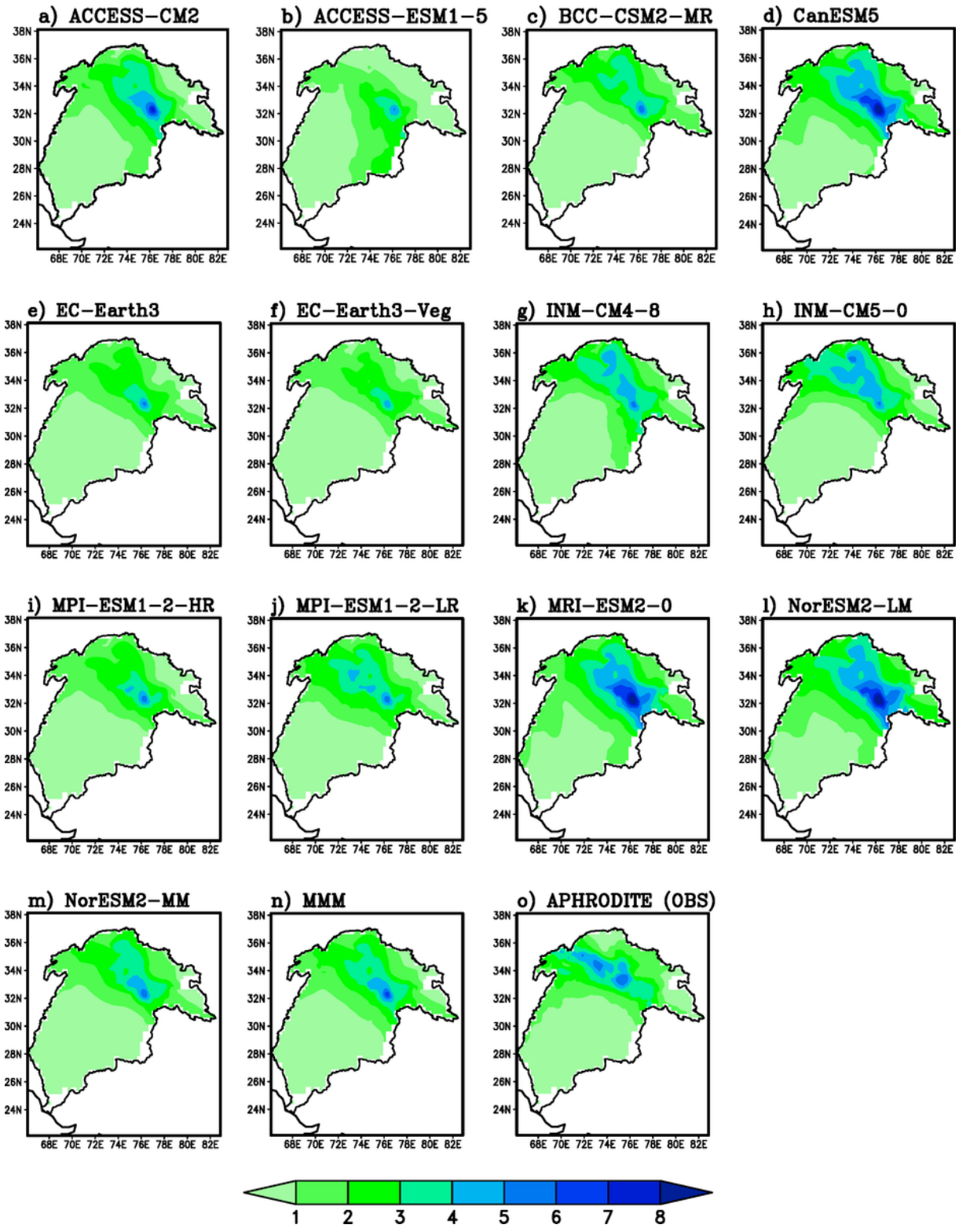

Figure 4

Same as Fig.3 but for winter season (DJF)

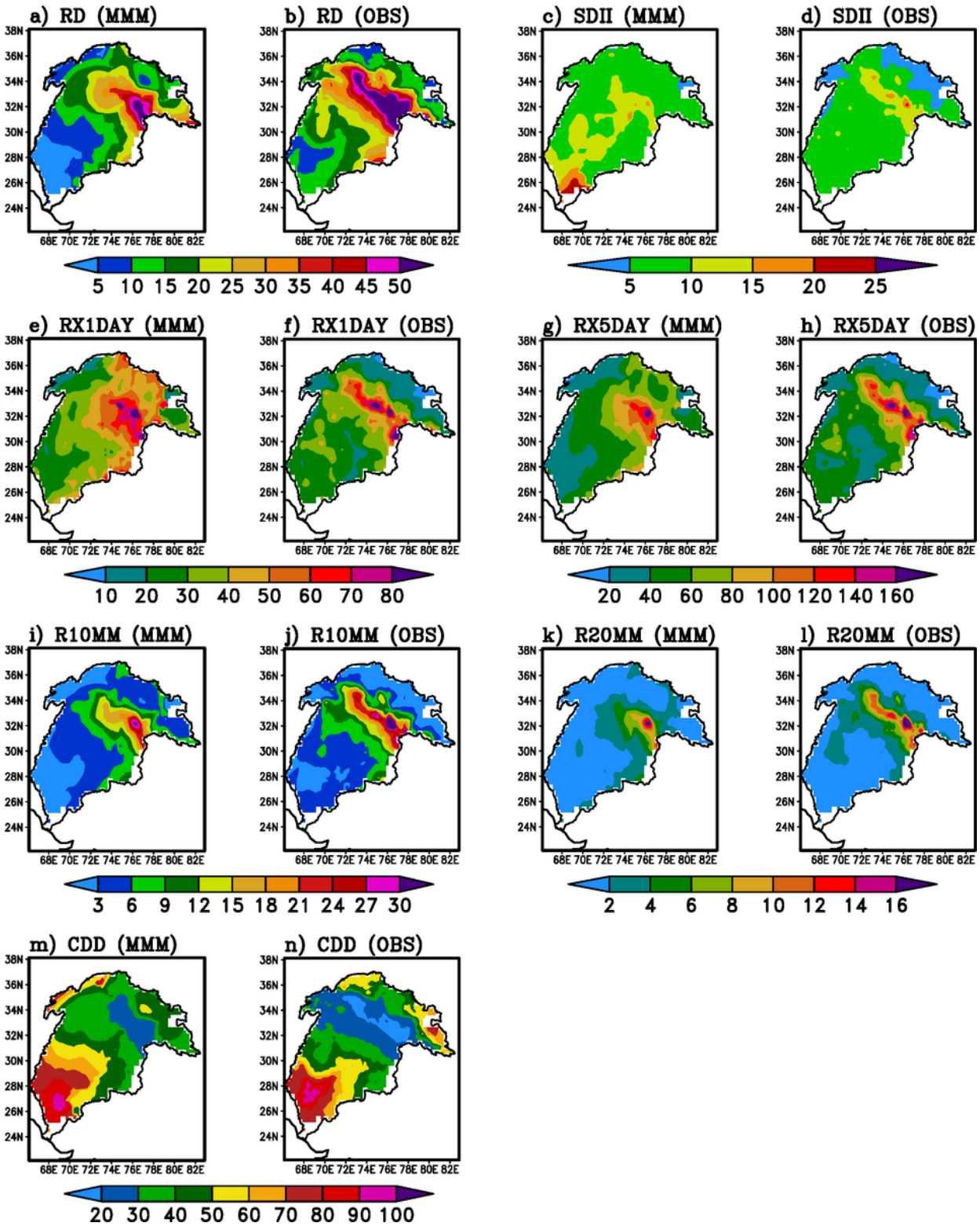

Figure 5

Spatial distribution of the precipitation extremes during summer monsoon (JJAS) season as captured by MMM of CMIP6 compared with the APHRODITE for the baseline period (1995–2014).

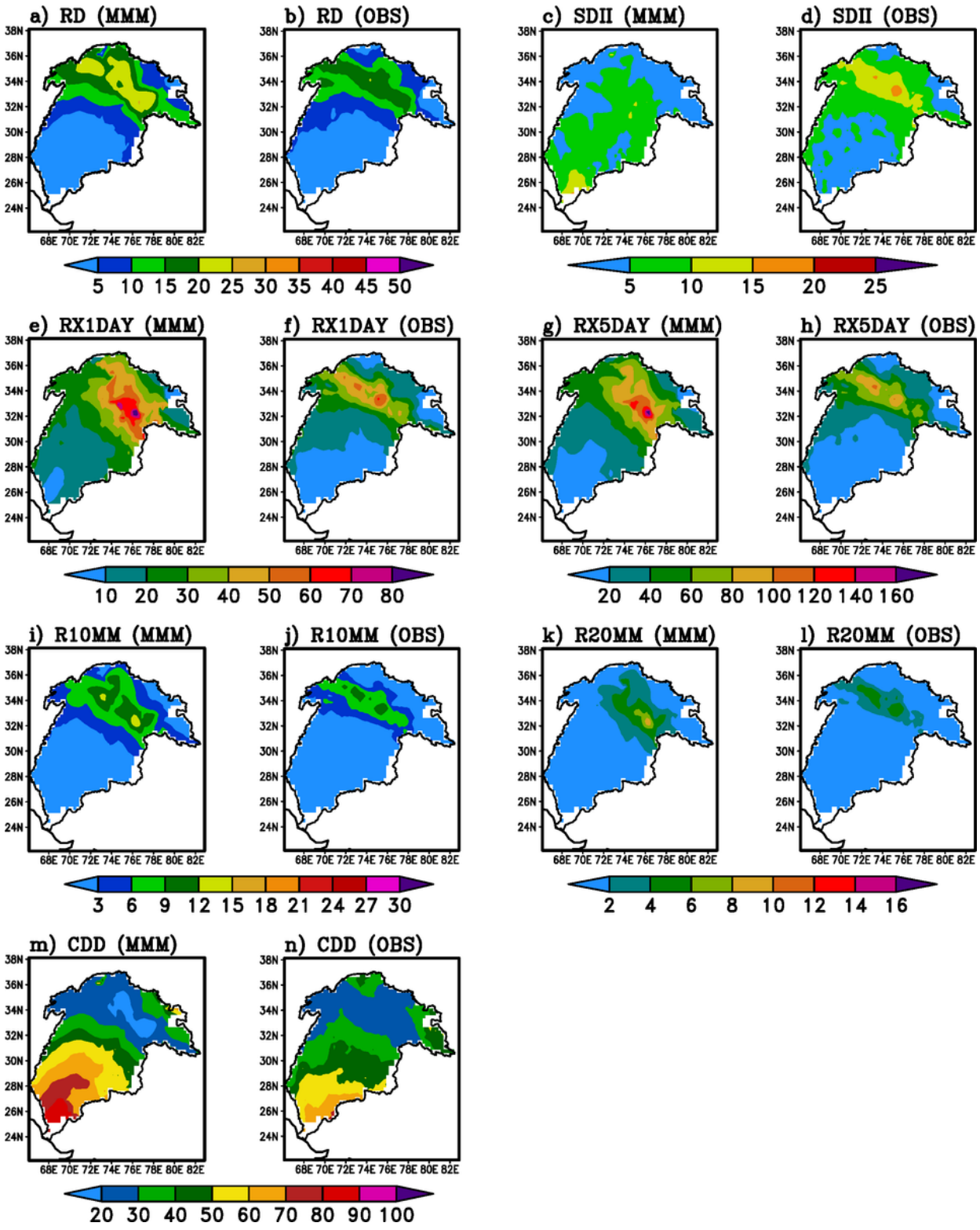

Figure 6

Same as Fig.5 but for winter season (DJF)

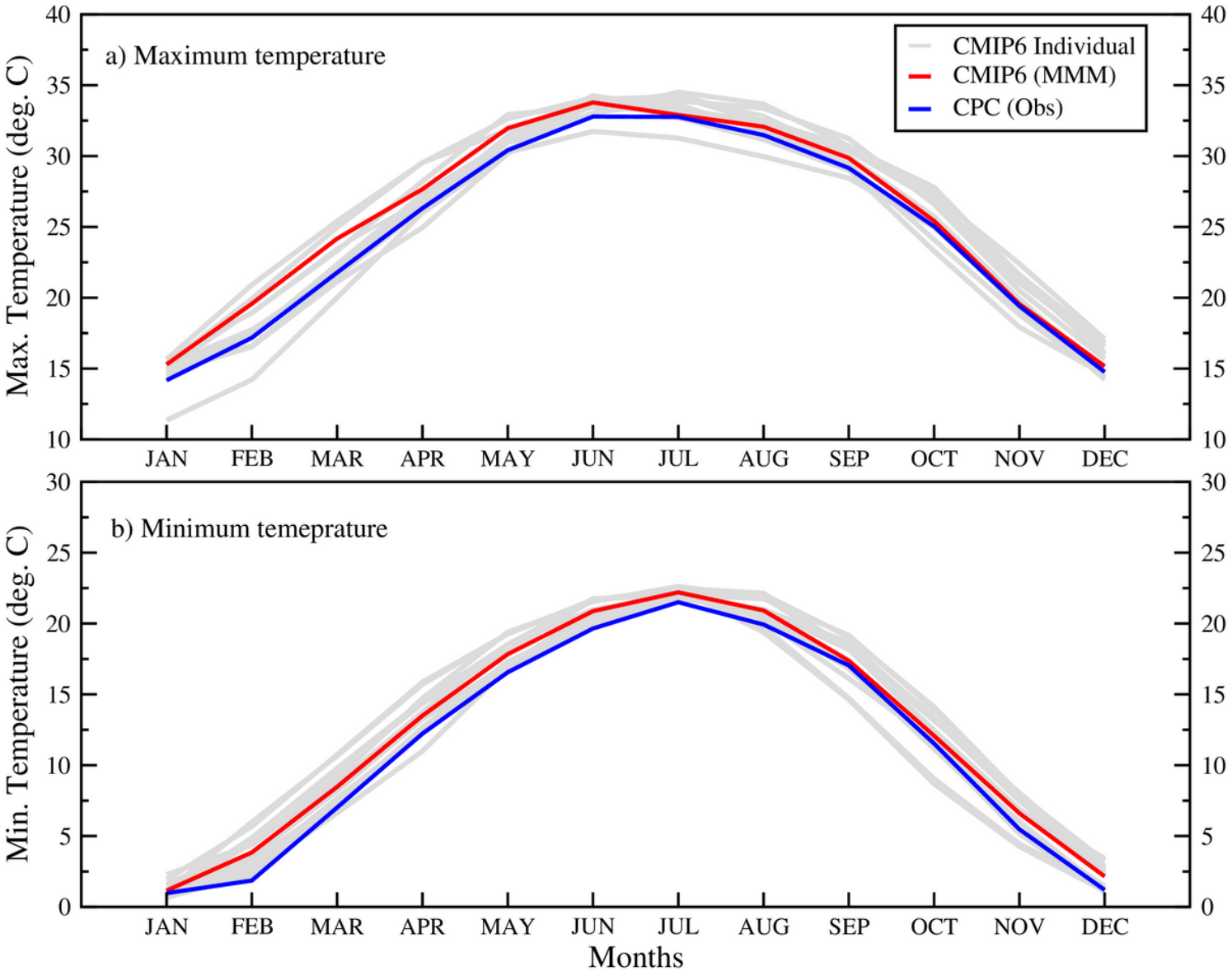

Figure 7

Annual cycles of monthly maximum and minimum temperature over the Indus basin from the CMIP6 models compared with CPC temperature data during the baseline period (1995–2014).

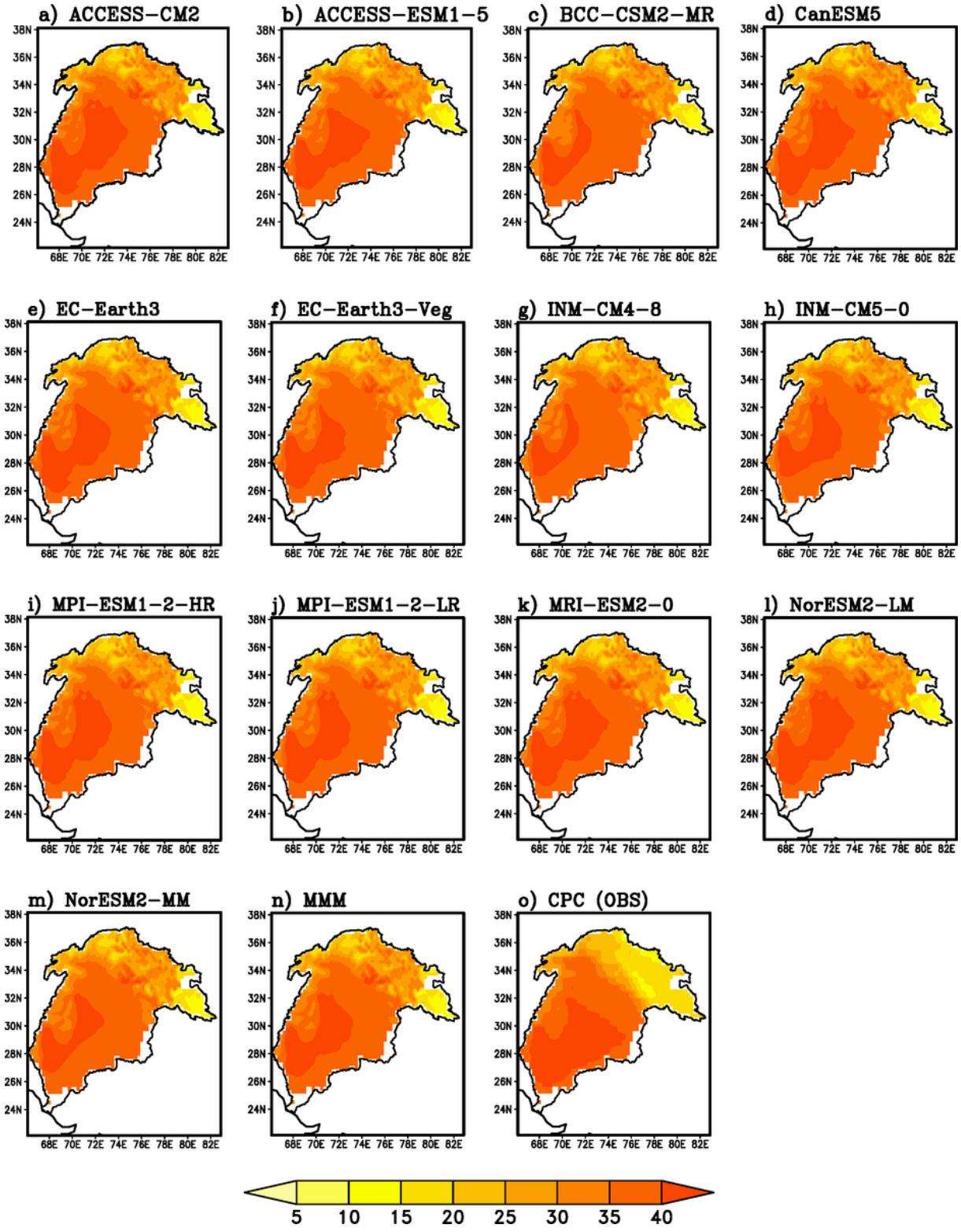

Figure 8

Spatial distribution of the summer season (JJA) maximum temperature (deg.C) as captured by CMIP6 individual models and their MMM compared with the CPC for the baseline period (1995–2014)

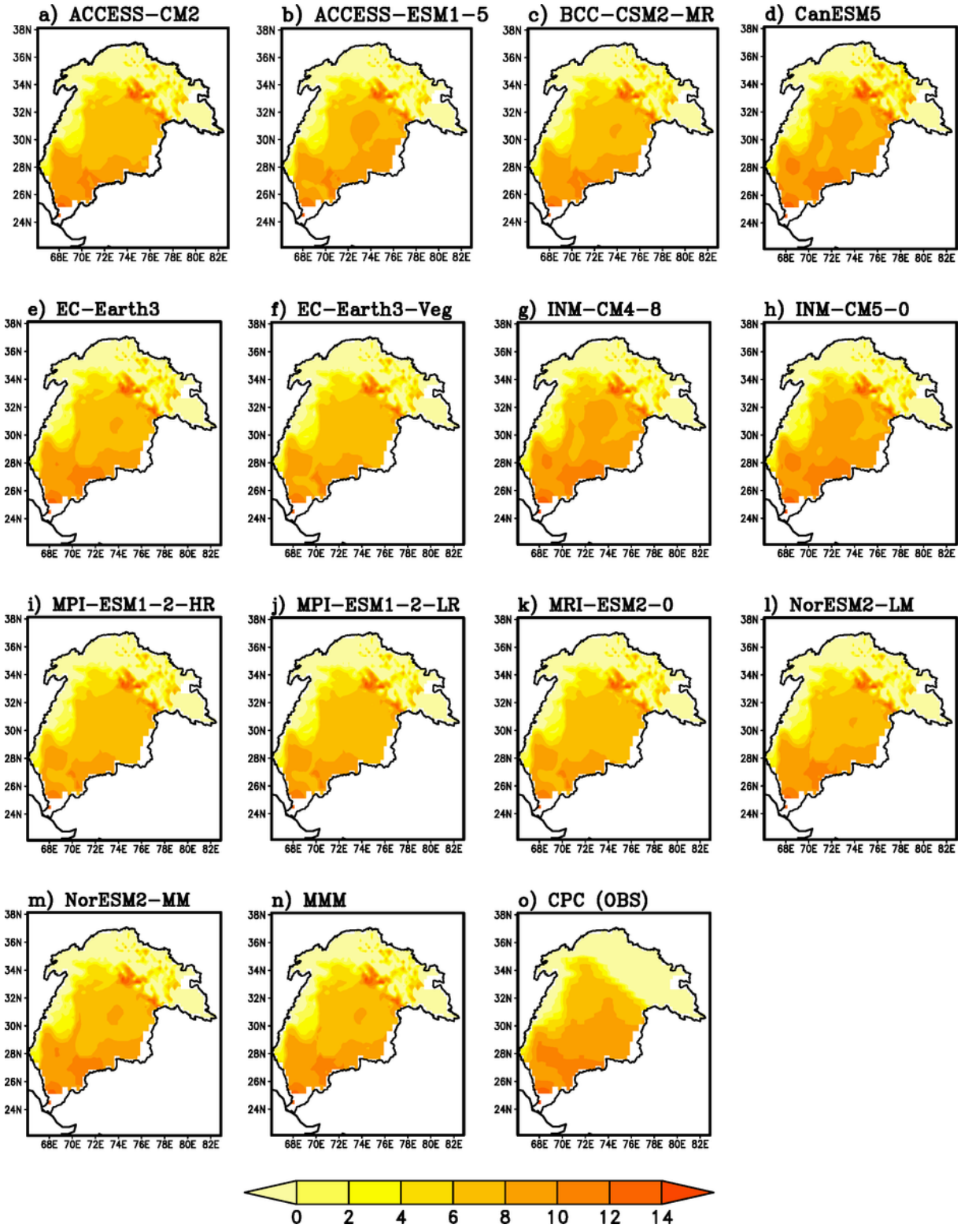

Figure 9

Same as Fig.11 but for winter season (DJF) minimum temperature.

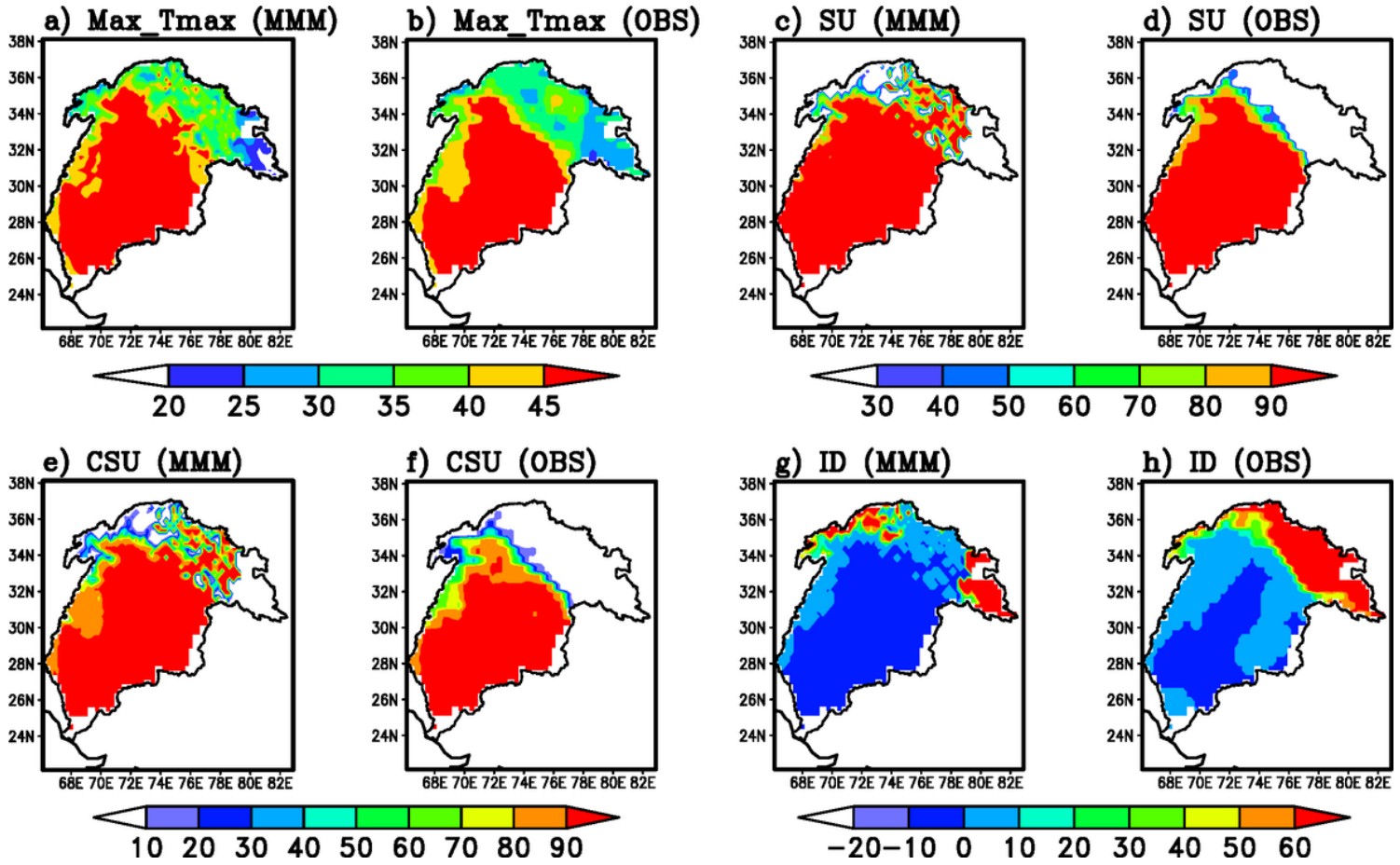

Figure 10

Spatial distribution of the maximum temperature extremes during summer season (JJAS) as captured by MMM of CMIP6 compared with the CPC for the baseline period (1995–2014).

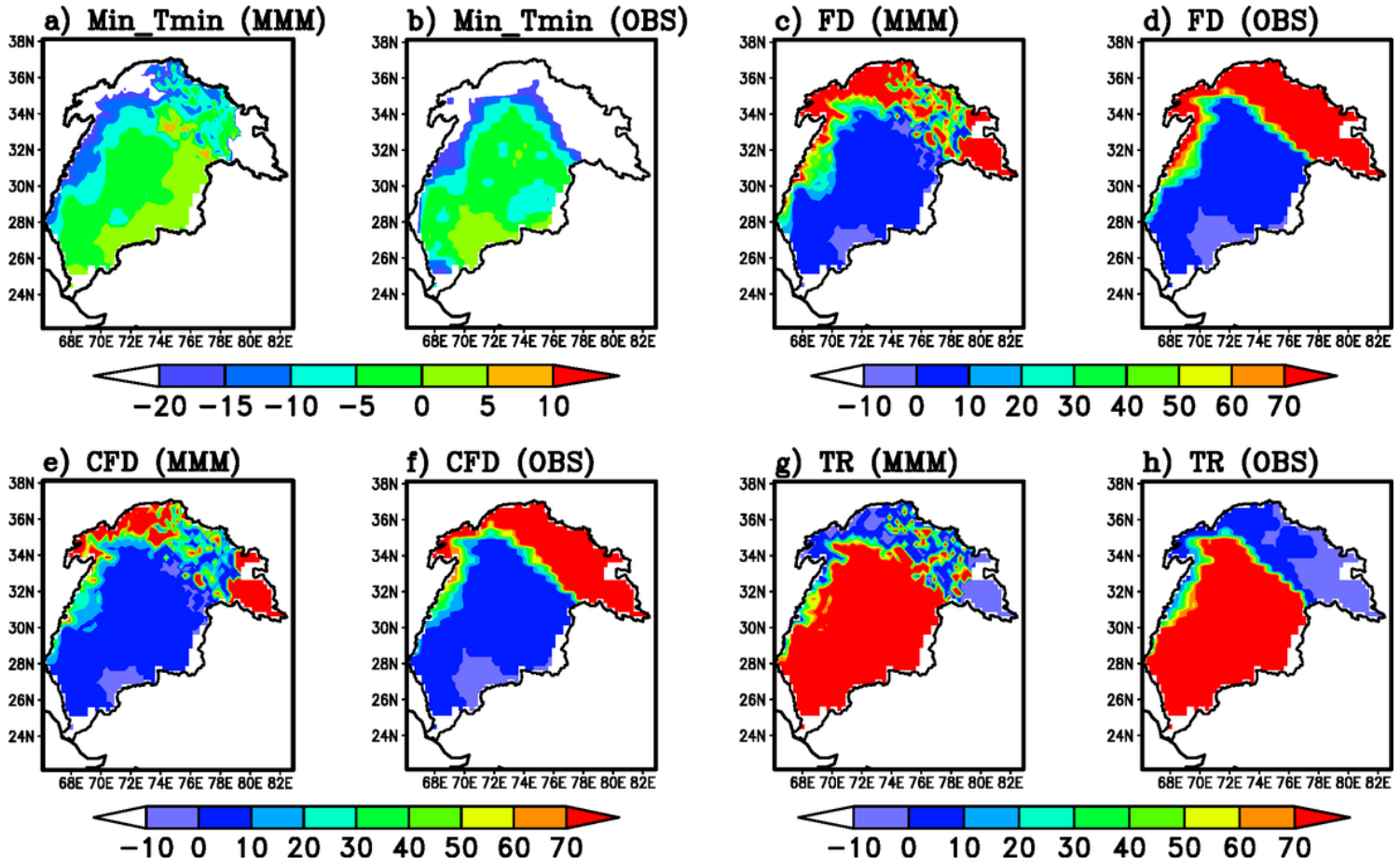

Figure 11

Same as Fig.13 but for winter season (DJF) minimum temperature extremes.

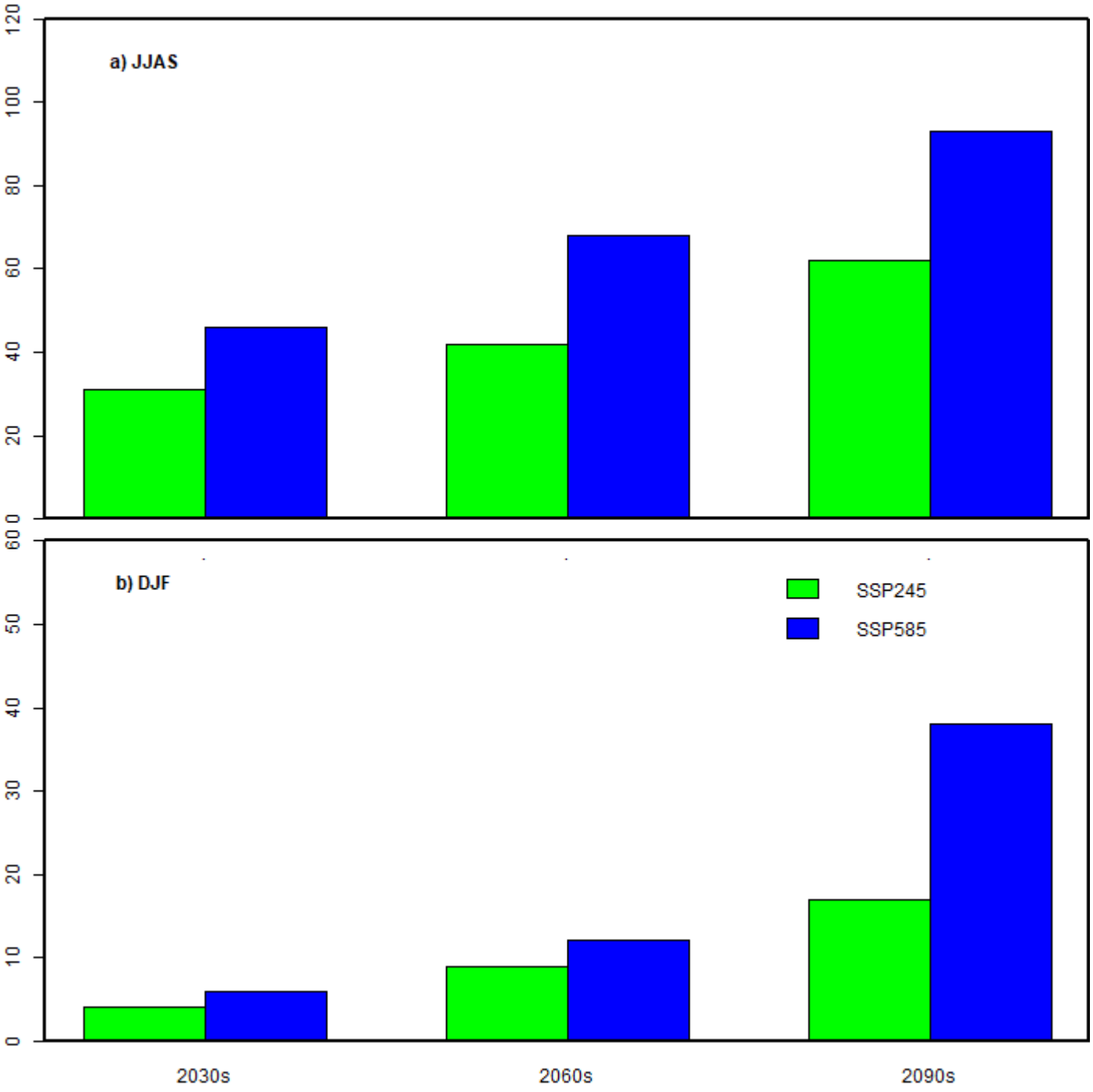

Figure 12

Projected changes in mean JJAS and DJF rainfall (%) from MMM of CMIP6 during 2030s (near future), 2060s (mid future) and 2090s (far future) with reference to the baseline 1995–2014.

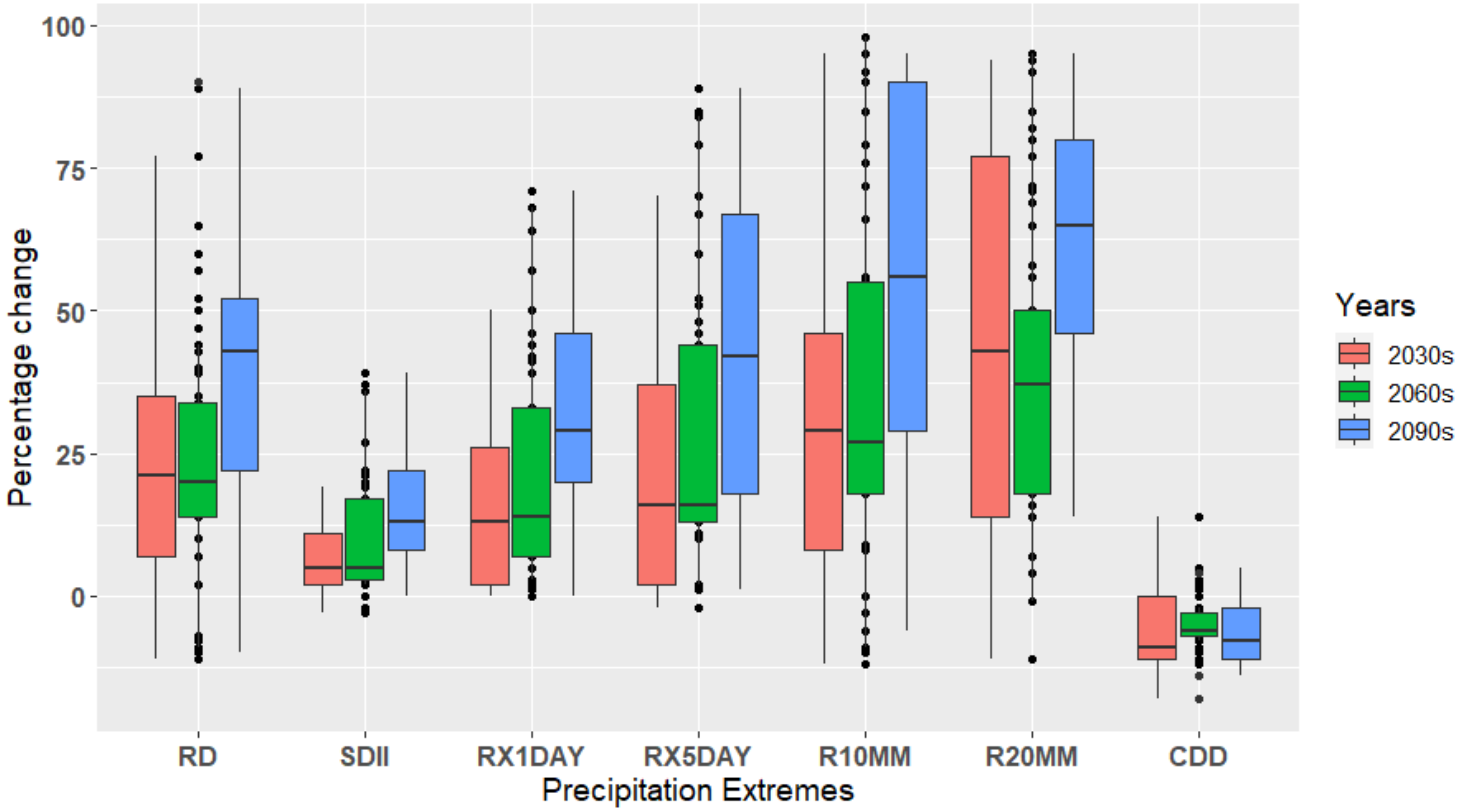

Figure 13

Projected changes different precipitation extreme indices during summer monsoon (JJAS) season from SSP2-4.5 of CMIP6 models during 2030s (near future), 2060s (mid future) and 2090s (far future) with reference to the baseline 1995–2014.

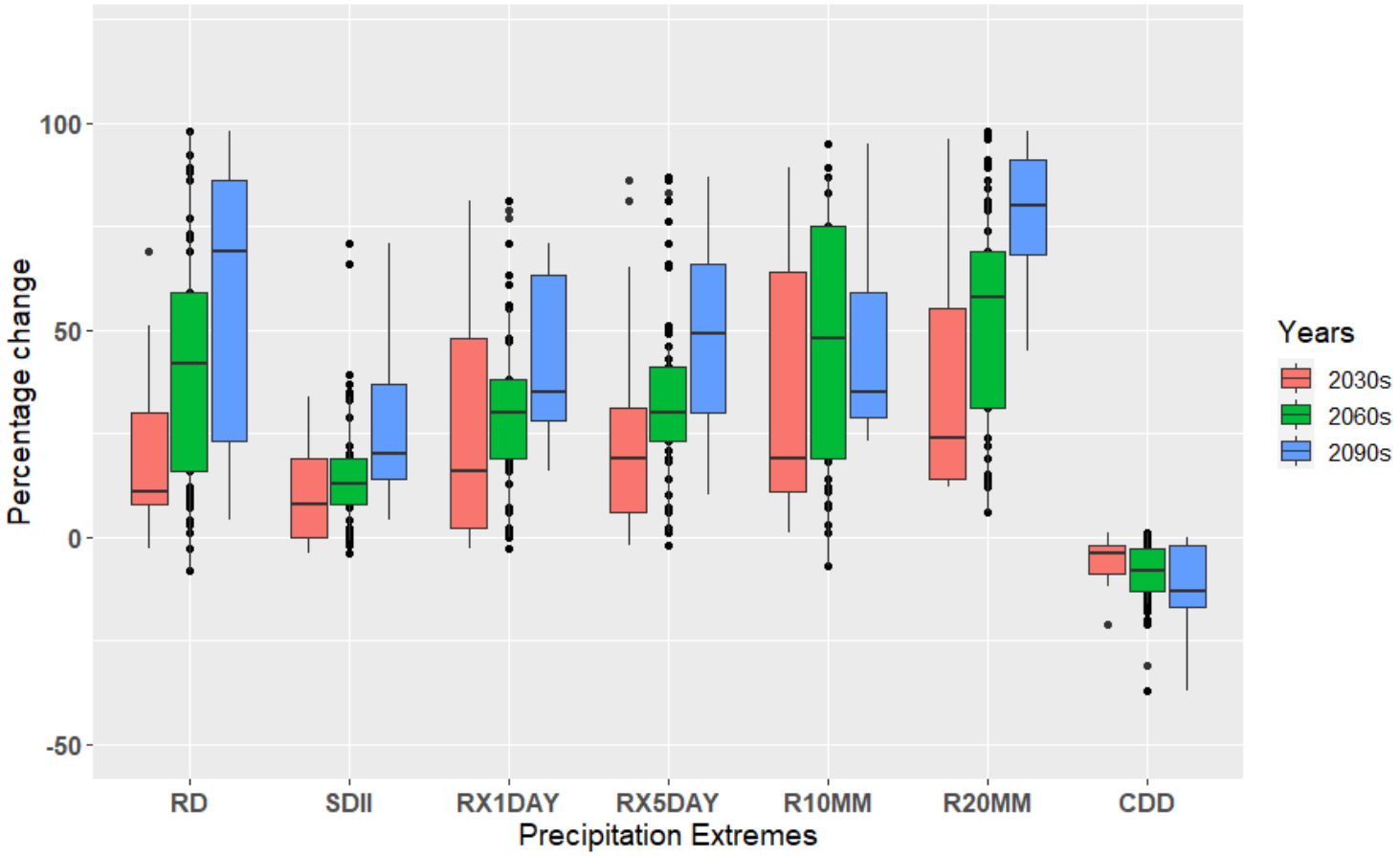

Figure 14

Same as Fig.8 but for SSP5-8.5

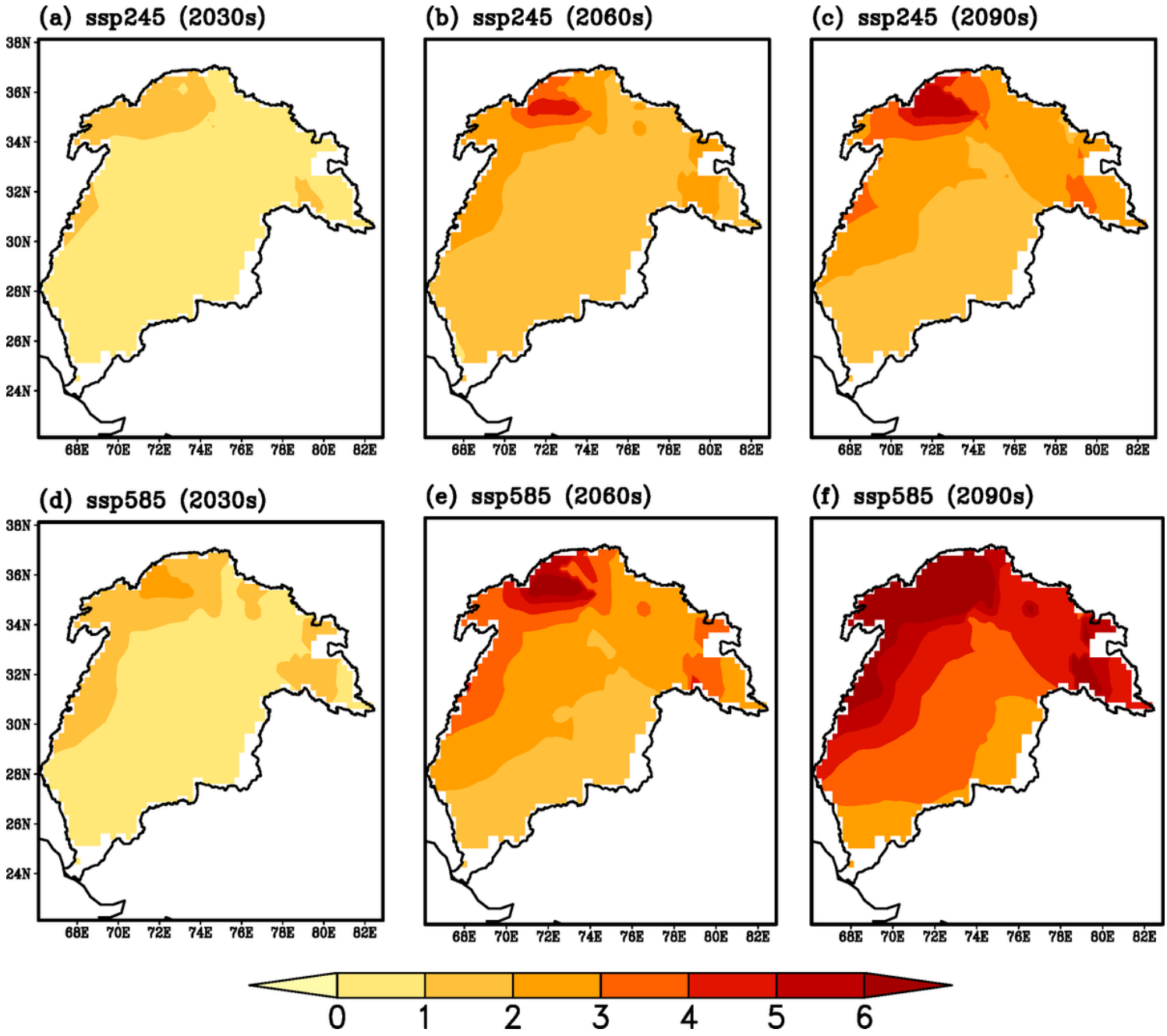

Figure 15

Projected changes maximum temperature during summer season (JJA) from SSP2-4.5 and SSP5-8.5 of CMIP6 MMM during 2030s (near future), 2060s (mid future) and 2090s (far future) with reference to the baseline 1995–2014.

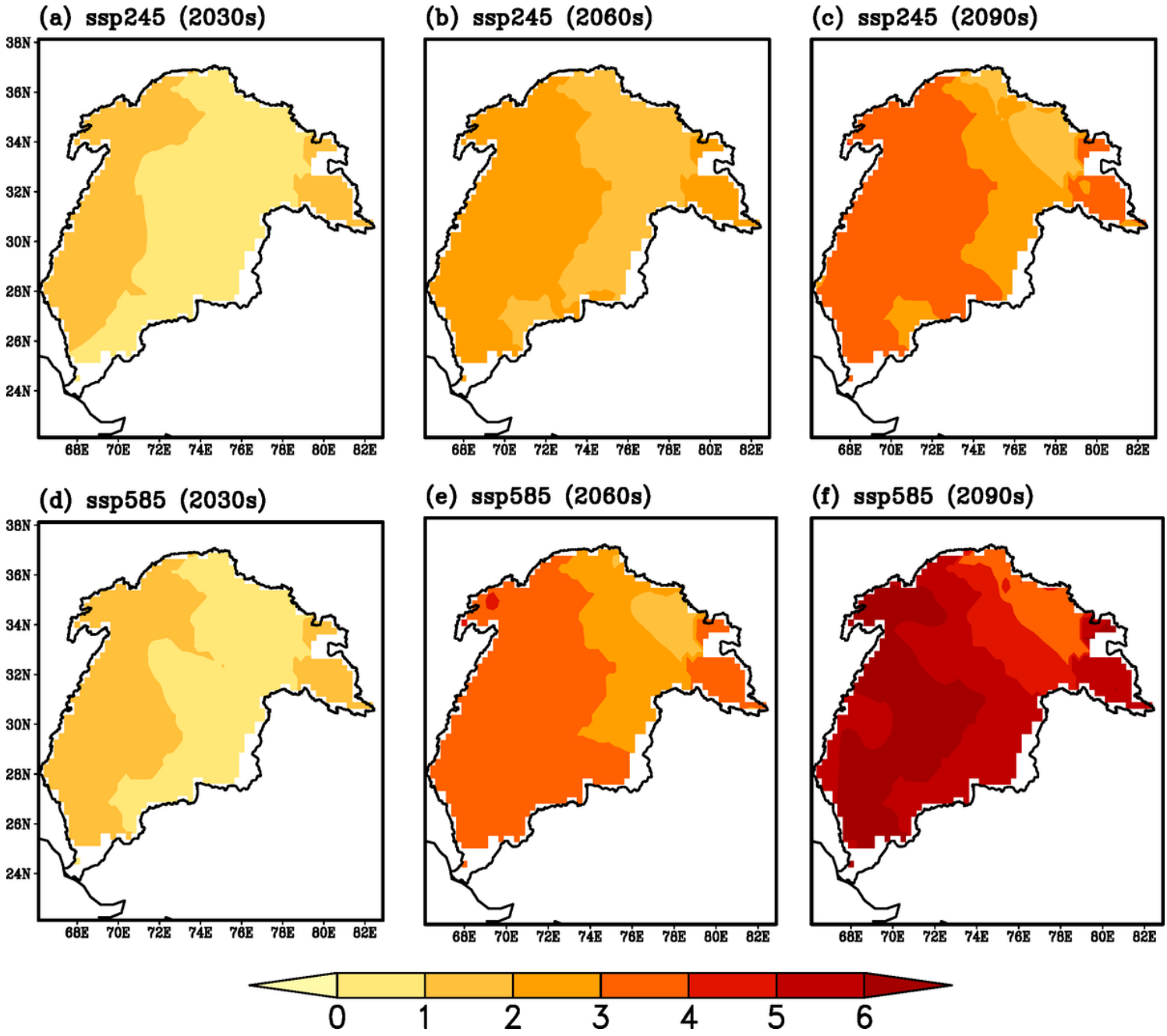

Figure 16

Same as Fig.15 but for winter season (DJF) minimum temperature.

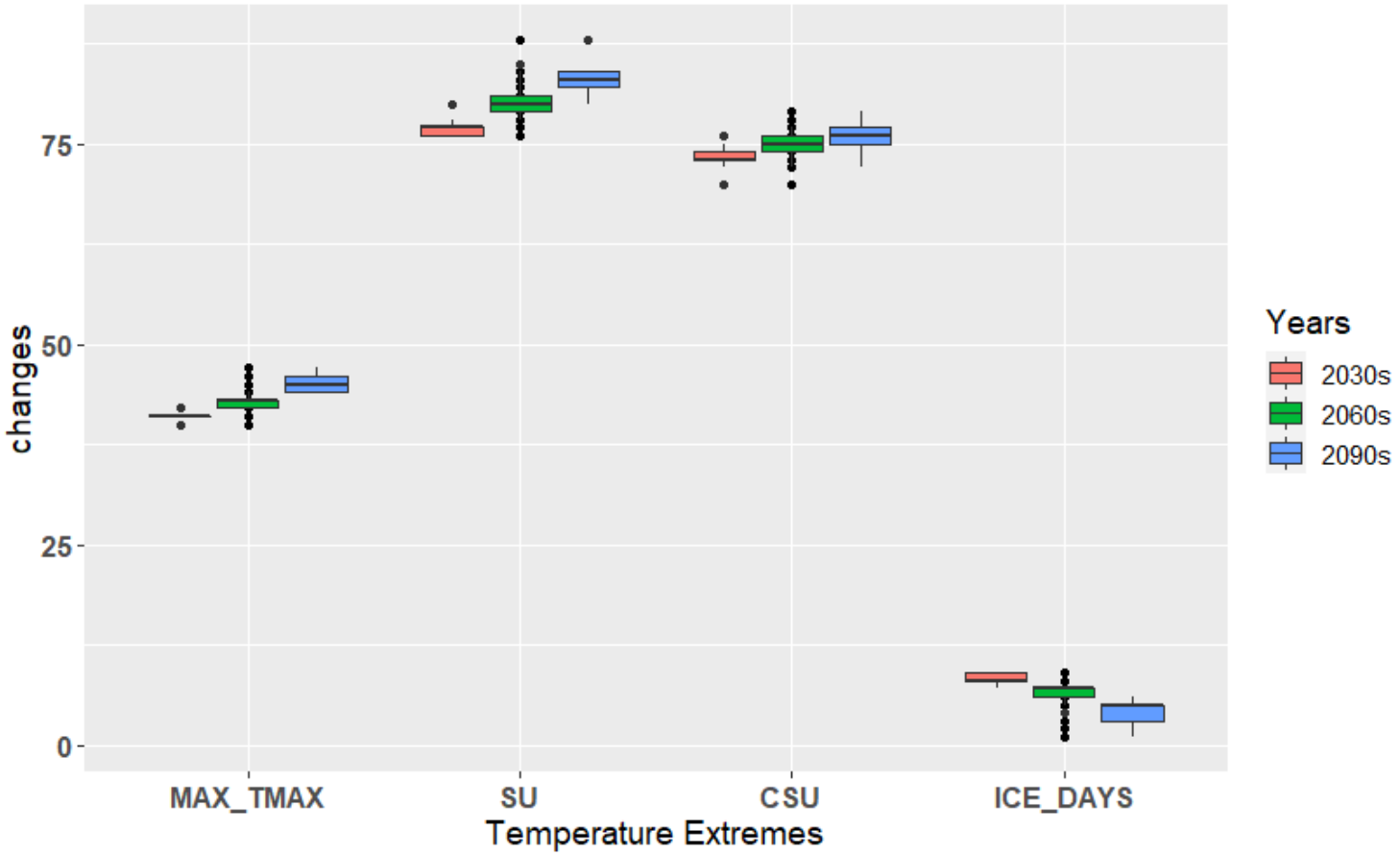

Figure 17

Projected changes different maximum temperature extreme indices during summer season (JJA) from SSP5-8.5 of CMIP6 models during 2030s (near future), 2060s (mid future) and 2090s (far future).

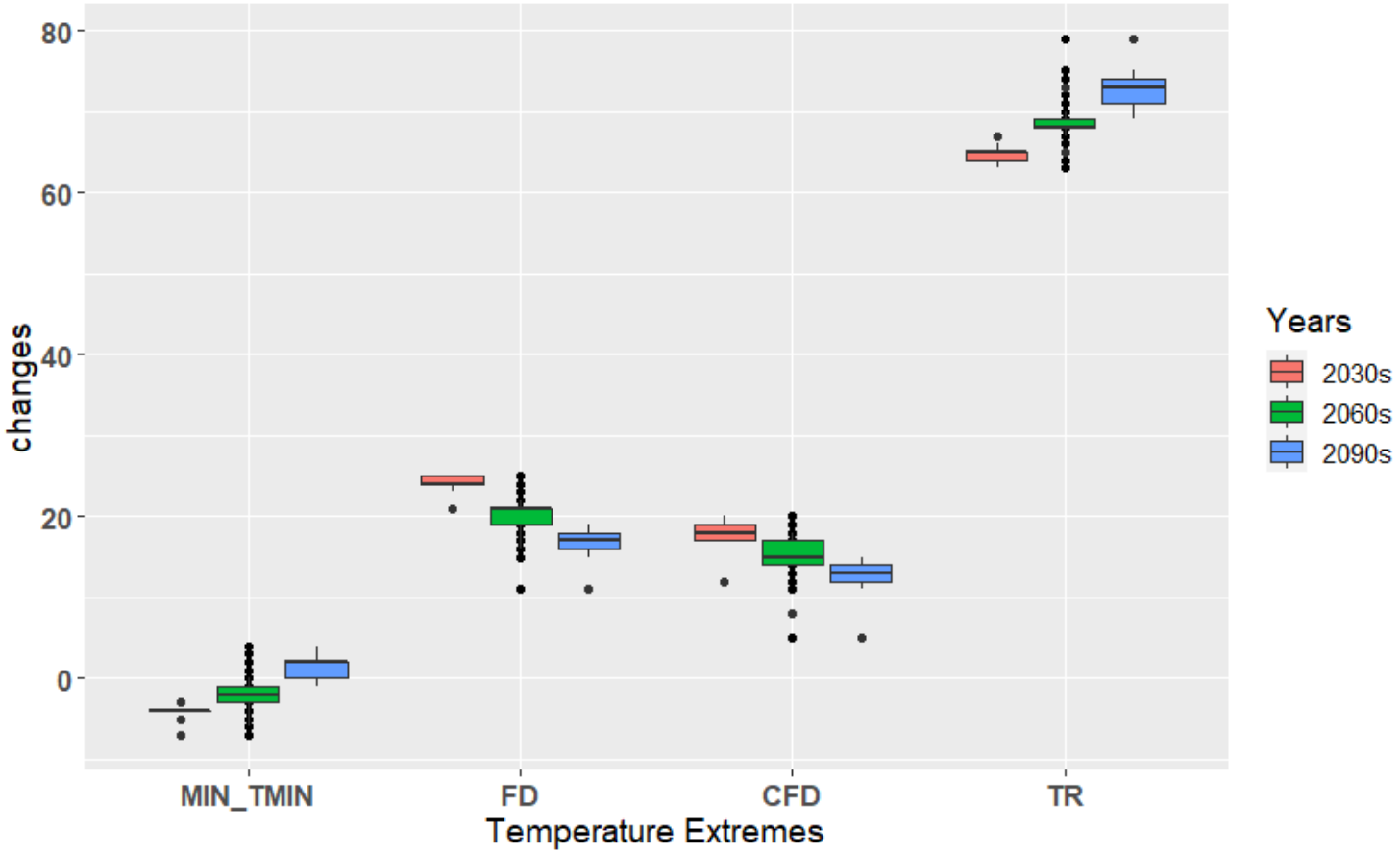

Figure 18

Projected changes different minimum temperature extreme indices during winter season (DJF) from SSP5-8.5 of CMIP6 models during 2030s (near future), 2060s (mid future) and 2090s (far future).